PHILOSOPHICAL TRANSACTIONS B

royalsocietypublishing.org/journal/rstb

Review

Cite this article: Tsvetanov KA, Henson RNA, Rowe JB. 2021 Separating vascular and neuronal effects of age on fMRI BOLD signals. *Phil. Trans. R. Soc. B* **376**: 20190631.
http://dx.doi.org/10.1098/rstb.2019.0631

Accepted: 19 May 2020

One contribution of 10 to a theme issue 'Key relationships between non-invasive functional neuroimaging and the underlying neuronal activity'.

Subject Areas:
neuroscience

Keywords:
neurovascular, cerebrovascular, cardiovascular, ageing, fMRI, cognitive function

Author for correspondence:
Kamen A. Tsvetanov
e-mail: kat35@cam.ac.uk

THE ROYAL SOCIETY PUBLISHING

Separating vascular and neuronal effects of age on fMRI BOLD signals

Kamen A. Tsvetanov[1,2], Richard N. A. Henson[3,4] and James B. Rowe[1,4]

[1]Department of Clinical Neurosciences, University of Cambridge, Cambridge CB2 0SZ, UK
[2]Department of Psychology, University of Cambridge, Cambridge CB2 3EB, UK
[3]Department of Psychiatry, University of Cambridge, Cambridge CB2 0SP, UK
[4]Medical Research Council Cognition and Brain Sciences Unit, University of Cambridge, Cambridge CB2 7EF, UK

KAT, 0000-0002-3178-6363

Accurate identification of brain function is necessary to understand the neurobiology of cognitive ageing, and thereby promote well-being across the lifespan. A common tool used to investigate neurocognitive ageing is functional magnetic resonance imaging (fMRI). However, although fMRI data are often interpreted in terms of neuronal activity, the blood oxygenation level-dependent (BOLD) signal measured by fMRI includes contributions of both vascular and neuronal factors, which change differentially with age. While some studies investigate vascular ageing factors, the results of these studies are not well known within the field of neurocognitive ageing and therefore vascular confounds in neurocognitive fMRI studies are common. Despite over 10 000 BOLD-fMRI papers on ageing, fewer than 20 have applied techniques to correct for vascular effects. However, neurovascular ageing is not only a confound in fMRI, but an important feature in its own right, to be assessed alongside measures of neuronal ageing. We review current approaches to dissociate neuronal and vascular components of BOLD-fMRI of regional activity and functional connectivity. We highlight emerging evidence that vascular mechanisms in the brain do not simply control blood flow to support the metabolic needs of neurons, but form complex neurovascular interactions that influence neuronal function in health and disease.

This article is part of the theme issue 'Key relationships between non-invasive functional neuroimaging and the underlying neuronal activity'.

1. Introduction

The worldwide population is rapidly ageing, creating a pressing need to understand the neurobiology of healthy cognitive ageing, over and above the problems associated with the rise of dementia in ageing societies [1]. Understanding the neural mechanisms of healthy ageing will inform efforts to maintain cognitive function, which is critical for well-being across the lifespan [2]. While neuroimaging has led to advances in knowledge about relationships between neural function and cognition, the effects of age on these interactions are poorly understood. This is owing in part to outdated methodology, inadequate awareness and treatment of confounding variables, opaque reporting of results, lack of replication and a failure to consider the limitations of the signals of interest. In this paper, we review two complementary disciplines, neurocognitive ageing and neurovascular ageing, which have suffered from these limitations and have proceeded somewhat independently. We argue for a better understanding of their relative contributions to functional magnetic resonance imaging (fMRI) signals, so as to formally integrate them in models of successful ageing, avoid common misinterpretations of fMRI and provide solutions to the limitations within each discipline alone.

The literature on neurocognitive ageing over the past 30 years has extensively relied on the blood oxygenation level-dependent (BOLD) signal

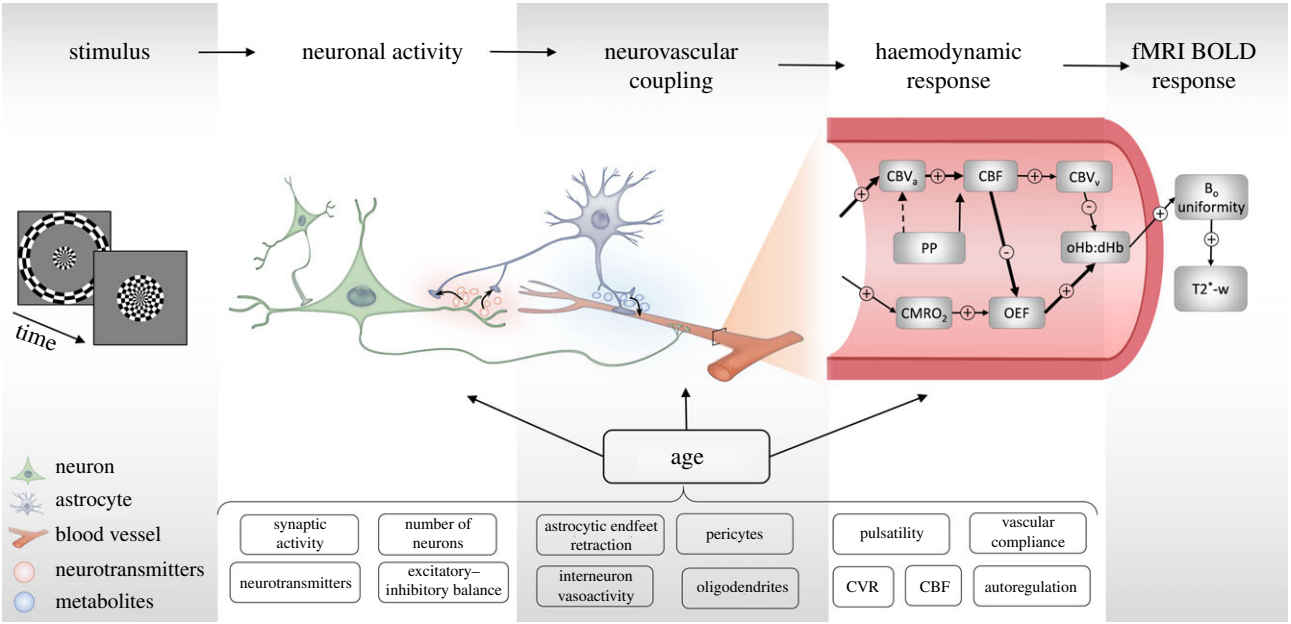

Figure 1. A schematic illustration of the physiological basis of the BOLD response. *Neuronal activity* elicited by a *stimulus* or background modulation gives rise to a complex *neurovascular coupling* signalling cascade. That triggers a *heamodynamic response* resulting in a blood-oxygen-level-depedent (BOLD) signal owing to changes in the magnetic field inhomogeneity detected as a T2*-weighted signal by an MRI scanner. (Lower panel) Some of the suspected mediators of the differential age effects on the processes that give rise to the BOLD response. CBV_a, arterial cerebral blood volume; CBV_v, venous cerebral blood volume; CBF, cerebal blood flow; CVR, cerebral vascular reactivity; $CMRO_2$, cerebral metabolic rate of blood oxygen consumption; oHb, oxygenated heamoglobin; dHb, deoxygenated heamoglobin; OEF, oxygen extraction fraction; B_0, magnetic field; PP, pulse pressure.

detected for most fMRI. The fMRI signal reflects changes in deoxyhaemoglobin concentrations in response to neural activity (figure 1). These concentrations change because increases in local synaptic activity and neuronal firing rates consume energy, which is sourced by transient local increase of cerebral blood flow (CBF) and cerebral blood volume (CBV). In simple terms, the dominant consequence is a temporary increase ('over-compensation') in oxygenated haemoglobin in the capillary and venous bed draining the activated region, reducing the concentration of deoxyhaemoglobin. Since deoxyhaemoglobin is paramagnetic, decreases in its concentration in turn increase the BOLD signal. The biophysical models of this *neurovascular coupling* include equations for dynamics of CBF, CBV and the cerebral metabolic rate of blood oxygen consumption ($CMRO_2$; for more details see [3–5]). The resulting BOLD changes to a brief (less than 1 s) period of neuronal activity that can last up to 30 s, with a characteristic temporal profile that is known as the *haemodynamic response function* (HRF) [6–9]. Many of the processes represented by parameters in these biophysical models are affected by ageing, owing for example to age-related changes in vascular health. Therefore, a failure to consider changes in vascular health can mean that differences in fMRI signals are erroneously attributed to neuronal differences [10–12] and in turn their cognitive relevance is misunderstood [13–15].

In this review, we first consider some of the main mediators of the transformation of neural activity into a haemodynamic response. We show how age-related alterations in the neuro–vascular interaction can influence the interpretation of changes in BOLD signal. This leads to changes in the measurements of regional activity and connectivity. We then turn to emerging evidence for the complex physiological changes with age, which give rise to slowing of cognitive function. These motivate the development of new models that characterize the joint contribution of vascular and neuronal influences to fMRI, in order to better understand the neurobiology of cognitive ageing. The continued interest in fMRI, above methods that are not affected by the vascular effects such as magneto- or electro-encephalography, rests on its safety, wide availability, high spatial resolution and full brain depth of imaging.

2. Age-related changes in neuro–vascular influences

The study of neurovascular pathology has been relevant to understanding many medical, neurological and psychiatric disorders. Alterations in the neurovascular system during healthy ageing have also been studied at both the cellular and structural levels. These changes typically remain undiagnosed and may have no directly apparent consequences for cognitive function, but they may compromise vasculature and the 'neurovascular unit' that couple neuronal activity to vascular responses. This undermines the straightforward interpretation of BOLD as an index of neurometabolic activity in older populations, those on drugs that influence vascular function and many diseases that alter the neurovascular unit. The following section reviews the major neurovascular changes related to ageing, and considers the physiological consequences of structural changes for the BOLD fMRI signal.

(a) Cellular and structural/morphological changes

(i) Vasculature, blood vessels and the cerebrovascular tree

Age leads to alterations in the cerebrovascular 'tree' at molecular, cellular and structural levels [16–19]. Large elastic arteries dilate, stiffen and become atheromatous and

tortuous, while the intima of the muscular arteries thickens [20]. Vascular stiffening is also associated with alterations in smooth muscle cells [21], calcification and disruptions in the collagen–elastin balance [22,23]. Some arterial alterations are coupled with capillary rarefaction, in addition to molecular and morphological changes that perturb the brain–blood barrier (BBB) [16,22,24]. Ageing is also associated with endothelial dysfunction, which contributes to dysregulation of vascular tone, astrocyte-dependent BBB permeability and nitric-oxide-dependent inflammation [19,25]. Damage to the endothelium aggravates vascular stiffening [22,26,27] and compromises the vessels' ability to dilate and constrict in response to variations of blood pressure or vasoactive substances [16,23]. In addition, there is an age-related impairment in the mechanism underlying electrical propagation of retrograde hyperpolarization signal along the endothelial cells, thereby impairing the remote vasodilation of upstream pial arterioles and increased perfusion in the capillary bed [25].

Pericytes are a group of microvascular mural cells embedded in the basement of blood microvessels that regulate blood flow both physiologically and pathologically [28] in addition to fine tuning vascular tone and BBB permeability with their contractile properties [29,30]. Age-related changes in pericytes [16,22] together with other mural cell alterations are likely to lead to changes in the vascular basis of the BOLD signal.

In short, disruption of a myriad of cerebrovascular factors acting on different levels of the vascular tree contributes synergistically to changes in neurovascular signalling, perfusion and reactivity.

(ii) Neuronal and non-neuronal cells

Neurons can directly control cerebral blood flow [31]. In particular, interneurons produce vasodilators [32,33] and vasoconstrictors [34], such as nitric oxide, prostanoids, endothelin etc. (for more information on vasoactive agents see [25,35]). Stimulation that selectively targets interneurons causes a relatively small increase in oxygen consumption but a relatively large increase in CBF. In contrast, stimulation of excitatory neurons causes relatively large increase in oxygen consumption but relatively small increase in CBF [36,37]. These results suggest that, while the primary driver of the BOLD response (i.e. CBF) is interneuron activation, additional $CMRO_2$-mediated changes in BOLD signal reflect excitatory neuron-modulated oxygen consumption [31]. The interpretation of these findings in the context of ageing is important, given the dissociating effects of age on excitatory versus inhibitory signalling and synapses [38–41].

While the role of glial cells in the neurovascular unit is less well understood than neuronal and vascular components, increasing evidence implicates glial elements as mediators between neurons and blood vessels [42]. Astrocytes are a diverse population of glial cells whose functions include neurovascular signalling [43], linking neurons to their blood supply [44] and regulating the BBB [45]. Activated astrocytes release vasoactive agents via multiple signalling pathways at different levels of the vascular tree [46] independently from other endothelial pathways [47] including caveolea-mediated vasodilation in arterial endothelium [48]. Retraction of the astrocytic endfeet as part of the clasmatodendrotic response [49], together with changes in the immune response and calcium signalling, impairs by-product clearance as the BBB efficiency breaks down [16,50]. Age-related changes in glia [16,22] together with mural and endothelial cell alterations could be stronger than that of neurons [51] and are likely to lead to changes in the vascular basis of the BOLD signal. Future work needs to consider how glial elements could be measured, integrated with *in vivo* neuroimaging and accounted for in physiological ageing models.

While both glia and neurons play a role in the vascular basis of the BOLD signal, their relative contribution to baseline (endogeneous) BOLD signal versus evoked (exogeneous, e.g. task-based) BOLD remains unclear. This is important because the baseline of blood flow, which decreases with ageing, can affect the sign and the magnitude of the evoked BOLD signal, without changes in underlying neural activity [52–55]. Age may differentiate the separate factors that regulate artery tone [31] versus evoked responses [36]. Taken together, it appears that subtypes of glia, mural cells, endothelium and inter-neurons control the BOLD signal, independent of the activity of the neighbouring excitatory neurons, and likely through multiple signalling mechanisms that contribute synergistically to vasodilation. Multiple neurovascular coupling (NVC) pathways acting on different levels of the vascular tree crucially depend on well-orchestrated interplay between different cell types of the neuro-glio-vascular unit, which may provide multiple safety mechanisms [46]. Ultimately, an integrated understanding of age effects on all components of the neuro-glio-vascular unit is required for a better understanding of the physiological basis of neurocognitive ageing, especially where inferences are drawn from fMRI.

(b) Physiological changes

It is the effects of age on cerebrovascular function that render interpretation of age differences in the BOLD signal so challenging. Cerebrovascular function can be assessed by measuring: (i) resting CBF, (ii) CBF responses to changes in arterial CO_2, referred to as cerebrovascular reactivity (CVR), (iii) CBF responses to changes in blood pressure, referred to as cerebral autoregulation, and (iv) CBF responses to changes in neural activation, referred to as NVC. Cerebrovascular alterations also include brain pulsatility and the cerebral metabolic rate of oxygen extraction. Below we review these changes based on the common range of physiological recordings (see also [16,25,56,57]).

(i) Resting cerebral blood flow

Decrease in global baseline CBF with age has been reported in early studies using transcranial Doppler ultrasonography [58], radiotracer techniques [56,59,60] and phase contrast imaging [61]. These changes are widespread across the cerebral cortex and the basal forebrain. The physiology underlying the CBF decrease in the aged brain is still debated [62]. The main candidates include primary causes of impaired vasoactivity and cardiovascular regulation of CBF during ageing, rather than the reduction in cardiac output [63]. CBF decline may also reflect the secondary effects of brain atrophy and reduction in neural activity as a shift towards lower metabolic demands, rather than primary changes in vasculature. The finding that changes in CBF can affect the sign and magnitude of the evoked BOLD signal without affecting underlying neural activity [52–54] is in line with the deoxyhaemoglobin-dilution model [64–66]. Therefore, the decline

in the baseline CBF with ageing has implications for the interpretation of fMRI studies of ageing.

(ii) Cerebrovascular reactivity

Cerebrovascular reactivity (CVR) is informative about vascular health. CVR is distinct from resting CBF, as it measures the ability of cerebral arteries and arterioles to dynamically regulate blood supply through dilation or constriction. In particular, CVR reflects the CBF responses to changes in arterial CO_2, whereby elevated partial pressure of arterial CO_2 (hypercapnia) causes dilation of vascular smooth muscle, leading to regional increases in CBF, while reduced CO_2 partial pressure (hypocapnia) causes vasoconstriction leading to regional decreases in CBF. Vascular sensitivity to CO_2 is very marked in the cerebrovasculature [67] and is thought to depend on intra- and extracellular pH changes that modulate vascular smooth muscle tone [68–70]. Therefore, CVR is considered to be a more direct measure of vascular endothelium and smooth muscle function compared to baseline CBF. CO_2 quantification in cerebrovasculature has used transcranial Doppler ultrasound [71], radiotracer techniques [72] and contrast imaging [73]. There is general agreement across multiple imaging techniques that changes in CBF relative to changes in CO_2 partial pressure are similar between brain regions under hypercapnia, but not under hypocapnia [74]. Experimental modulation in CO_2 partial pressure has been used to validate non-invasive perfusion techniques [75,76], as well as biophysical [77] and biochemical [78] aspects of cerebral vasodilation.

Global decline in CVR with age has been reported using transcranial Doppler ultrasound [58], radio tracer techniques [60,79,80] and phase contrast imaging [81]. Age-related differences in the response of regional CBF to CO_2 inhalation have been reported using PET [82]. Reduction in hypercapnia-induced vasodilation in the cerebellum and insular cortex, as well as hypocapnia-induced vasoconstriction in the frontal cortex, has been observed in older adults, suggesting less effective vascular response in cerebral perforating arteries [82]. Likely causes for CVR changes are arterial stiffening [83] and compromised endothelial function in blood vessels [84], which lead to a decreased vascular response to match metabolic demands. In addition, white matter hyperintensities, a common MRI finding in ageing, are associated with reduced baseline CBF and reduced response to hypercapnia [85,86]. Compromised CVR will lead to a reduced dynamic range of the BOLD signal, having direct implications for task-based fMRI studies of ageing: even with the same levels of neural activation across age groups, lower CVR in the older group would lead to smaller amounts of vasodilation and therefore reduced evoked CBF, reduced decrease of deoxyhaemoglobin concentration and reduced BOLD signal. Without controlling for CVR differences, this would lead to an under-representation of neural responses in older individuals.

(iii) Pulsatility

Cyclic cardiac contractions that pump blood through the arterial system generate a pulsatile blood flow and concomitant pulsatile pressure experienced by vascular wall tissue. This pulsatile phenomenon is absorbed before it reaches pressure-sensitive cerebral capillaries, and maintenance of steady flow and pressure ensures exchange of nutrients and clearance by-products. The first line of defence to minimize the effect of flow and pressure pulsatility in the microcirculation is achieved by the highly elastic aorta and muscular arteries, e.g. the aorta–carotid interface. The distensibility mismatch in these vessels dampens the pulsatile energy projected distally, known as the Windkessel effect [87,88]. Arterial stiffening caused by imbalance in elastin–collagen in the load-bearing intima of the aorta and central elastic arteries alters arterial distensibility, translating into increased pulse wave velocity [89]. The change of pulse wave velocity with age alters the wave reflection properties at the aorta–carotid interface, resulting in less effective cushioning of pulsations in the arterial system, i.e. diminished Windkessel effect, and greater transmission of pulsatile energy into the cerebral microcirculation [56]. Increase of pulsatility in the proximal part of cerebrovasculature is further exacerbated with age increase in pulse pressure (increased difference between systolic and diastolic pressure). Transcranial Doppler ultrasound of major arteries entering the brain, together with phase contrast MRI of the whole brain, both point to an age-related increase in cerebral pulsatility [90,91]. These changes can potentially contribute to microvascular ischaemia and tissue damage that is seen in some MRI-derived measures [90,92,93]. These microvascular changes have in the past been considered as a benign feature of ageing, but may actually be a significant contributor to changes in neurocognitive function [94]. With regards to BOLD imaging, pulsatile blood flow not only leads to fluctuation in signal intensity in arteries, arterioles and other large vessels [95], but also an age-related increase in pulsatility deeper in microvasculature. This could have dramatic effects on the BOLD signal in the proximity of neuronal tissue, which has only recently been recognized as a potential confound of BOLD studies [12,96–100].

(iv) Cerebral autoregulation

The second line of defence for minimizing pressure fluctuations in brain microvasculature is cerebral autoregulation, referred to here as autoregulation, via the vessels' ability to dilate or constrict in response to systemic perfusion pressure changes [74]. This is complementary to CVR [101,102]. In particular, autoregulation constitutes the ability of the cerebral vasculature to maintain steady flow and pressure in the capillary bed during transient changes in arterial pressure or intracranial pressure. The myogenic response, which is intrinsic to the vascular smooth cells and a key mechanism to autoregulation, is impaired with ageing, especially under conditions of hypertension and increased pressure pulsatility [57]. Furthermore, impaired autoregulation precedes vascular damage in white matter [103] and relates to white matter hyperintensities [104] in animal and human studies, respectively.

The CVR and autoregulation adjustment of vascular resistance to varying arterial CO_2 and pressure, respectively, is primarily modulated in large arteries and pial arterioles [74]. This suggests that BOLD-related measures targeting CVR and autoregulation may be sensitive to ageing effects in the proximal part of the vasculature, and less sensitive to independent changes in the distal part of the cerebral circulation and physiological factors therein. In other words, CVR and autoregulation may be less sensitive to mechanisms underlying retrograde intramural propagation of vascular

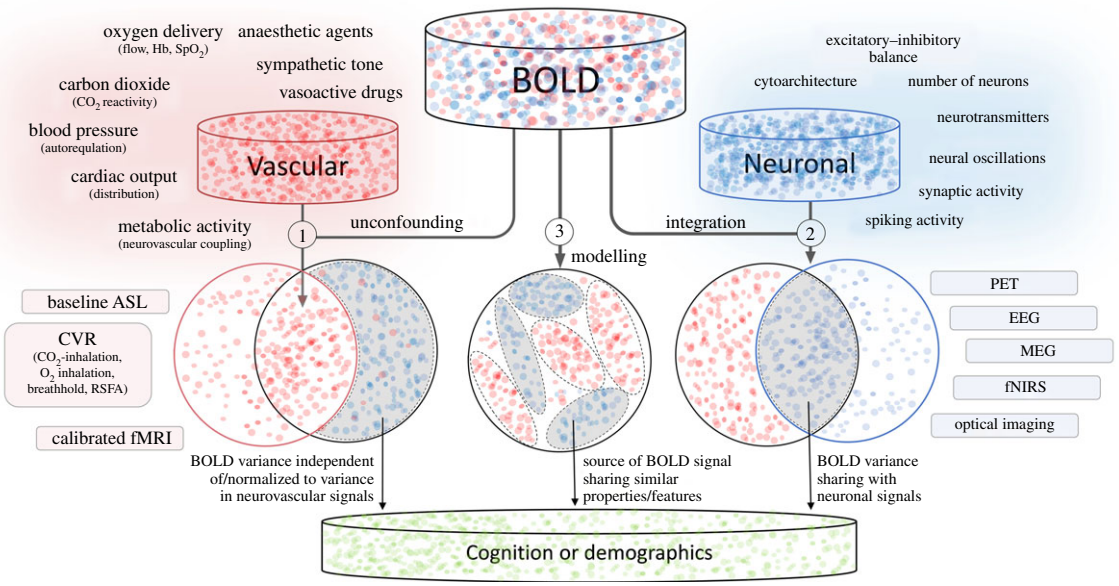

Figure 2. Schematic illustration of dissociating neurovascular influences in fMRI-BOLD using (1) vascular unconfounding, (2) neuronal integration and (3) BOLD modelling. ASL, arterial-spin labelling; EEG, electroencephalography; fNIRS, functional near-infrared spectroscopy; MEG, magnetoencephalography; PET, positron emission tomography; RSFA, resting state fluctuation amplitude.

signals, causing remote vasodilation of upstream pial arterioles, i.e. impairing mechanisms of communication within the neurovascular unit [47].

(c) Drug effects

Older people are more likely to be taking medications, including medications for age-related chronic disorders such as high blood pressure, diabetes, blood clotting, arthritis or neurodegeneration. Ageing studies often do not explicitly address these potential confounds in the interpretation of their results, which potentially modifies their conclusions, especially since the drugs are likely to affect the cascade of signalling and vascular events that form the basis of the BOLD signal [105]. Approaches aimed at dissociating vascular from neuronal signals should seek to identify, characterize and control for the confounding effects of drugs in ageing studies.

3. Dissociating neuro–vascular influences in BOLD fMRI signal

In order to interpret fMRI data, one needs to understand the contributions of neuronal and vascular components of signal variance. Some studies of neurocognitive ageing attempt to bypass the impact of vascular influences through their inclusion criteria, e.g. excluding individuals with a history of hypertension, cardiovascular or neurological conditions. These are, however, categorical criteria that are insensitive to continuous variation in the population and unable to resolve the effects of undiagnosed/presymptomatic conditions, not to mention producing results that are potentially biased in not generalizing to the typical ageing person.

There are several other approaches to separate, or 'unconfound', neural from vascular factors. These are summarized as three broad strategies (figure 2). The first is based on detecting vascular signals in BOLD fMRI data by using independent measurement of vascular signals, termed here *vascular unconfounding*. The second relies on identifying neuronal signals in BOLD fMRI by using independent measurement of neuronal signals, termed *neuronal integration*. The third uses formal *modelling approaches* to the fMRI signal. Below we review the methods and exemplar applications within each strategy, and illustrate their strengths and weaknesses for studying the effects of ageing.

(a) Vascular detection using fMRI

The first class of approaches focuses on estimating vascular contributions to the BOLD signal using an independent MRI-based measurement that aims to capture individual variability in one or more of the physiological factors discussed in the previous section. An implicit assumption of these methods is that they explain variability in vascular signals (see figure 2), but not variability related to neural activity, such that they can be used to 'adjust' the BOLD signal without removing age-related neuronal changes. These approaches further fall into calibration and normalization methods. We focus here on task-evoked BOLD responses in voxel-wise imaging, but the principles can be applied to other forms of analysis.

(i) Normalization using baseline cerebral blood flow

Regional baseline CBF has for many years been measured with positron emission tomography (PET) [106] or MRI using tracer kinetic procedures [107]. However, safety concerns associated with tracers and the complexity of procedures have limited their application in BOLD studies of ageing. The predominant fMRI method for estimating resting CBF is based on endogenous contrast generated through perfusion of blood water into brain tissue [108]. The signal intensity is generated by applying a magnetic label to proton spins of the inflowing arterial blood water, termed arterial-spin labelling (ASL) [109]. In analogy to PET perfusion imaging, the ASL 'tracer' is the endogenous arterial

blood water, where the magnetic label decays with T1 instead of radioactive decay. Deep understanding of the physiological basis of ASL and validation against radiotracer approaches [110–115] has established ASL as a robust and non-invasive technique to provide quantitative estimates of baseline CBF. An overview of ASL-variations and an agreement on its application have been discussed previously [116].

Resting state ASL studies of ageing support the presence of age-related atrophy-independent decreases in resting CBF throughout the cortex [117–119]. Some studies also suggest a nonlinear effect across the lifespan [120]. Interestingly, increases in regional CBF, in lateral and medial temporal lobe for example, have been observed with increasing age [118,121,122], which may reflect macro-vascular artefacts [123,124] owing to prolonged arterial transit time with ageing [125].

ASL studies support the proposal that age-related decline in baseline CBF reflects both cardiovascular and neurovascular impairment [119]. For example, age-related reduction in baseline CBF occurs in cortical regions typically associated with high vascular risk and genetic factors [126,127], and precedes brain atrophy [128–130]. However, recall that baseline brain perfusion is highly dependent on other physiological factors, and the difference in CBF may also reflect age bias in these factors, rather than baseline changes in CBF [131]. For example, baseline ASL may reflect spontaneous CO_2 fluctuations, medication use, time of day, or levels of wakefulness [132]. Some influences are global and related to vascular tonus, while other local variations are the result of psychotropic effects on the brain. As an example, physical exercise, drinking coffee or smoking just before the perfusion measurement have substantial influence on both global and local quantification [133–136]. While this may be a drawback for absolute CBF quantification, it is an advantage for the use of ASL as a normalization technique, i.e., to control for multiple physiological factors in BOLD studies.

ASL has been broadly used to estimate baseline CBF, and has been used to try to rule out drug effects on vascular contributions to BOLD effects of disease or drug [137,138]. However, it is rarely used for a formal normalizing approach in evoked BOLD studies of age. This could be owing to the low signal-to-noise ratio of ASL, low spatial resolution and additional time needed to acquire baseline CBF, and a preference to integrate it within a BOLD fMRI acquisition (see §3a(iii) below). In one study, regional age-related differences in BOLD activation were shown to be mediated by baseline ASL-CBF, suggesting a substantial vascular contribution with regional specificity to the observed BOLD age differences [139]. In summary, the improvement in quality and application of baseline ASL-CBF measurements in recent years offers advantages over some of the other following approaches to control for age-related differences in physiological influences of BOLD signal.

(ii) Normalization using cerebrovascular reactivity

This approach differs from the baseline perfusion approach in that it relies on experimentally perturbed physiological states during the MRI scan. This physiological response, defined as cerebrovascular reactivity above, leads to changes in BOLD signal that are dominated by vascular factors (reflecting transient variations in physiological factors) in the absence of apparent changes in neuronal activity. In particular, estimation of cerebrovascular reactivity exploits the molecular mechanisms of CO_2-induced vasodilation (discussed in §1b above), which can be used to model variability in physiological signals of evoked BOLD data. Fluctuations in arterial blood CO_2 can take three forms of hypercapnia: CO_2 administration, voluntary breathhold or naturally occurring fluctuations linked to respiration during a resting state fMRI acquisition (discussed in 3a(ii) and in [140]). As the CVR manipulations work under the assumption of no changes in the underlying neuronal activity and oxygen extraction ($CMRO_2$) [64], the CVR manipulation takes the form:

$$\Delta\mathrm{BOLD}_{\mathrm{CVR}} = M(1 - f_{\mathrm{CVR}}^{\alpha-\beta}),$$

where $f = \mathrm{CBF}/\mathrm{CBF}_0$ represents CBF signal normalized by its respective baseline value. The subscript CVR denotes the hypercapnia condition and the parameter M defines the maximum possible BOLD signal change for a brain region. The superscript parameters are determined empirically, but are well approximated as $\alpha \approx 0.4$ and $\beta \approx 1.5$ [6]. Dividing the task-based BOLD response by the hypercapnia response yields a normalized BOLD response of the form:

$$\Delta\mathrm{BOLD}_N = \frac{(1 - f_F^{\alpha-\beta} m_F^{\beta})}{(1 - f_{\mathrm{CVR}}^{\alpha-\beta})},$$

where $m = \mathrm{CMRO}_2/\mathrm{CMRO}_{2,0}$ represents $CMRO_2$ signal normalized by its respective baseline value. The subscripts N and F denote the normalized BOLD response and the functional responses, respectively. Note that the M term cancels out in the normalized response, which precludes estimation of modulatory factors of M, such as magnetic field strength and baseline blood volume and oxygenation [141]. This normalization procedure entails the division of a functional contrast map by a CVR map, i.e. normalization at each voxel. However, including the hypercapnia response as a covariate in a voxel-level, general linear model (GLM), together with the functional BOLD response (e.g. when predicting behavioural or demographic measures) might provide a better approach [142]. It is worth noting that these operations assume a linear relationship between CBF and BOLD signal that holds across varying CO_2-levels in arterial blood. However, this may not always be true [143], given claims of a nonlinear BOLD–CBF relationship [144] and a nonlinear response of vasculature to large CO_2 and arterial pressure fluctuations [101,145]. This is further complicated by the 'vascular steal' phenomenon of flow diversion from regions of low to high cerebrovascular reactivity [146] and interactions between multiple physiological factors that increase with age [22]. While this warrants future research on modelling the nonlinear nature of the effects, the current approaches may lead to underestimation, rather than overestimation, and therefore still offer a partial solution to minimize vascular influences in evoked BOLD signal.

CO_2-induced hypercapnia

An individual's hypercapnia response can be modulated by inhaling a special gas mixture inside the MRI scanner. Bandettini and Wong [141] were the first to demonstrate the utility of this technique for BOLD fMRI studies. (For a technical review and practicalities of this approach using various types of apparatus, see Liu *et al*. [140,147] and Germuska & Wise [148].) Regardless of the gas-delivery apparatus,

accurate assessment of CVR relies on tracking the maximal concentration of CO_2 in the exhaled air—so-called 'end-tidal CO_2' (Et-CO_2)—during breathing cycles with varying CO_2 concentration in the inhaled gas (see in video format, [149]). The variation of Et-CO_2 is tightly linked to changes in alveolar pressure of CO_2 and fluctuations in arterial vasodilation, indicating the extent to which the vascular system is challenged. The analysis of CO_2-induced hypercapnia data is conceptually similar to the task-evoked fMRI, where the temporally aligned Et-CO_2 timecourse is included as the main regressor in a GLM to produce a cerebrovascular response (CVR_{CO_2}) brain map. Early studies of CO_2-induced cerebrovascular reactivity demonstrate a close regional overlap between voxels showing BOLD CO_2 responses (BOLD-CVR_{CO_2} map) estimated from fMRI and voxels showing a cerebrovascular response (CBF-CVR_{CO_2} map) estimated from PET [150] and ASL [143,151,152]. Although this overlap has high reproducibility [153] across various field strengths and MRI sequences [154], BOLD-CVR_{CO_2} is more sensitive to basal CO_2 fluctuations than CBF-CVR_{CO_2} [143].

BOLD-CVR_{CO_2} in grey matter declines with age [11,152,155–157]. The age effects on BOLD-CVR_{CO_2} are more prominent than those on baseline ASL-CBF [155,156] and exhibit distinct regional patterns [117], supporting the notion of age having independent effects on CVR and baseline CBF [118]. Interestingly, age-related BOLD-CVR_{CO_2} increases are found in white matter [157], which may reflect changes in the mechanical properties of the white matter: white matter in older adults becomes less densely packed owing to demyelination and axon loss, making it easier for blood to penetrate and vessels to dilate.

Combining BOLD-CVR_{CO_2} with evoked BOLD studies of ageing allows correction for regionally specific effects [11,158], which could lead to improved associations between BOLD estimates and outcomes of interest [159]. For example, age-related decreases in evoked BOLD responses in V1 and medial temporal lobe were abolished after correction, while age-related increases in bilateral frontal gyrus remained after correction. This suggests that many age-related differences found in fMRI studies reflect changes in vasodilation rather than in neuronal activity.

Unfortunately, such corrective methods have not been widely used, in part owing to impracticalities of large-scale studies, and tolerance by older adults and clinical populations [160,161]. Furthermore, a gas-induced hypercapnic challenge may not be neuronally neutral [162–165], e.g., given participants' awareness of the aversive challenge, and this effect on neural activity may differ with age [166]. In this case, correction by CVR_{CO_2} might obscure true task-related neural differences with age. Nonetheless, recent developments in the gas challenge procedure allow for estimation of multiple physiological parameters, including venous oxygenation and resting state functional connectivity (see [167]), which may improve the accuracy of corrections for vascular signals in BOLD fMRI studies.

Breath-hold-induced hypercapnia

An alternative way to modulate arterial CO_2 in the absence of gas-delivery apparatus involves breathing challenges, where participants endogenously increase arterial CO_2 by voluntarily holding their breath [168], which we term CVR_{BH} to indicate breath-holding [169]. BOLD-based CVR_{BH} demonstrates high correspondence with ASL-based CVR_{BH} [170,171], BOLD-CVR_{CO_2} ([172–174]; cf. [175]) and has excellent repeatability [176,177]. Improved CVR_{BH} estimation may be achieved using variations in the breath-hold procedure [178–181] and in analysis of the data [176,182,183].

Beyond its use to minimize inter-individual variability of physiological influences in BOLD studies of young adults [142,172,174,184–187], breath-holding has been used more commonly in ageing studies than other normalization approaches [172,188–194]. Riecker and colleagues showed that the age differences in BOLD response of sensorimotor regions during finger tapping were accompanied by differences in BOLD-CVR_{BH} [194], which was one of the first indications that evoked fMRI studies of ageing require careful interpretation of observed BOLD differences. Later studies extended these findings to other primary sensory regions, and corroborated the idea that age-related decline in evoked BOLD response to sensorimotor stimuli can be accounted for by age differences in CVR_{BH} [172,191]. Interestingly, age differences in BOLD signal in 'higher-order' cortical regions during cognitive tasks often remained after controlling for CVR_{BH}, suggesting the relationship between BOLD signal, neural activity, vascular signal and age varies across brain regions [172,191]. More recent studies confirm that consideration of CVR_{BH} not only changes the pattern of regional age differences in evoked BOLD response [188,192,195], but also improves the strength of the relationship between BOLD responses and performance on the task [196].

However, while breath-holding may be more tolerable and has been employed in more ageing studies than gas-induced CVR, the compliance to the breath-holding procedure, lung capacity, inspiration and expiration ability of participants may decrease with their age [197]. Such biases affect data quality and reliability measures [175,179], highlighting the advantage of other less invasive (task-free) estimates of vascular components of BOLD time series.

Resting state fluctuation amplitudes

One such 'task-free' estimate of the vascular component of the BOLD signal is the intrinsic variability of the BOLD signal across time (after bandpass filtering to remove slow drifts in MRI signal and high frequency motion artefacts). This is known as resting state fluctuation amplitude (RSFA). Early studies demonstrate that RSFA reflects naturally occurring fluctuations in arterial CO_2 induced by variations in cardiac rhythm and in respiratory rate and depth [198,199]. RSFA approximates the BOLD response to hypercapnic challenge and was proposed as a safe, scalable and robust cerebrovascular reactivity mapping technique [12,200]. As with other methods discussed above, the use of RSFA as a correction method for BOLD requires the assumption that age differences in RSFA reflect only vascular factors, rather than age-related differences in neural function. Although RSFA demonstrates high correspondence across brain regions and individuals when compared to baseline ASL-CBF [118,201], BOLD-CVR_{BH} and BOLD-CVR_{CO_2} [197,200,202], and in groups with compromised CVR [203,204], the effects of age on RSFA cannot be fully explained by these factors [118,201]. Therefore, without understanding the unexplained effects of age on RSFA in terms of neuronal versus vascular influences it would be dangerous to use RSFA as a normalization technique.

Recent evidence has improved our understanding of the origins of RSFA. For example, pulsatile effects could influence the BOLD signal in the proximity of large brain vessels and cerebrospinal fluid. In particular, the age-related increase in pulsatility deeper in microvasculature (see *Pulsatility* §2b(iii)) is likely to contribute to the RSFA signal, as recently recognized [12,96–100]. This could explain why Tsvetanov and colleagues [12] found that age differences in RSFA are either fully or partly mediated by heart rate variability. In contrast, these authors further found no evidence that neural variability (as measured by magnetoencephalography (MEG)) mediated the age effects of RSFA [12]; these findings were further supported by EEG-based neural estimates [205]. However, while age-related differences in RSFA may not reflect neuronal signals, the use of either somatic vascular measures or cerebrovascular measures explained only part of the age-related differences in RSFA. This leaves open the possibility that age-related differences in RSFA reflect joint contributions from cardiovascular and neurovascular factors, as in the case of BOLD signal fluctuations [206,207].

To resolve this ambiguity, we followed up our original study by considering the simultaneous assessment of the independent and shared effects of cardiovascular, cerebrovascular and neuronal effects on age-related differences in RSFA [118]. After controlling for either cardiovascular and neurovascular estimates alone, the residual variance in RSFA across individuals remained significantly associated with age, replicating the above findings. However, when controlling for both cardiovascular and cerebrovascular estimates, the residual variance in RSFA was no longer associated with age. This suggests that cardiovascular and cerebrovascular signals are together sufficient predictors of age-related differences in RSFA. In summary, while originally proposed to control for CVR [200], RSFA captures multiple vascular signals that are independently affected by age, and appears to be a valid method to correct for vascular factors in the BOLD signal, in order to better characterize effects of age on neural, and ultimately cognitive, function.

When RSFA is used to correct evoked BOLD data, the amplitude and spatial pattern of the normalized response are similar to that when using CVR_{BH} and CVR_{CO_2} [200]. Controlling for RSFA has been shown to minimize non-neural BOLD variability across individuals [186] in populations with impaired cardiovascular health [208,209], and improve estimation of evoked BOLD signals related to distinct neuronal mechanisms [210]. In studies of ageing, controlling for RSFA in evoked BOLD signal accounts for age-related differences in BOLD response in some sensory regions, comparable to findings from alternative normalization approaches [12,190,191,211]. Importantly, not all age differences disappear after controlling for RSFA—for example, the ipsilateral motor cortex overactivation in older adults remains, consistent with results from other approaches used to study ageing effects on the motor system [212–215].

Variations in the estimation of RSFA exist, which may be more sensitive to CVR relative to cardiovascular signals [216]. In addition, other means of RSFA-like estimates have been proposed to derive from non-resting cognitive states [217] or fixation-/resting-periods succeeding task periods [201]. Given that short periods of cognitive engagement have been shown to modulate the BOLD signal in a subsequent resting state scan [218,219], future studies are required to generalize RSFA findings to RSFA-like estimates derived from other types of fMRI acquisitions.

Other CVR-induced variations

The measures discussed above could be complemented with other physiological measures, such as total baseline venous oxygenation from phase contrast MRI [220], which may provide superior signal-to-noise ratio compared to ASL, or cerebral blood volume [114] with multiple physiologic parameters [221]. Their usefulness for estimating age-related differences in the vascular component of the BOLD signal remains to be demonstrated.

(iii) Calibration using concurrent fMRI

The use of so-called 'calibrated fMRI' has been possible for many years and can in theory control for differences in both baseline physiology and haemodynamic coupling across individuals and hence ages. The technique involves measuring blood flow, blood volume and venous oxygenation via normocapnic and hypercapnic/hyperoxic gas challenge during a concurrent measurement of BOLD and CBF [148,222,223]. As such, calibrated fMRI provides a measure of relative changes in $CMRO_2$, which can be integrated with physiological models [224,225], to estimate quantitatively the absolute rate of cerebral metabolic oxygen consumption ($CMRO_2$), i.e. oxidative metabolism, from the data. However, it has not seen widespread adoption, mainly because it is difficult to implement.

In theory, measurements of task-evoked oxidative metabolism provide quantitative estimates of $CMRO_2$, which can help understand neuronal differences in oxidative metabolism across age groups even if they have differences in vascular health [10,158,226–228]. However, for at least some of this work, the motivation has been to distinguish the physiological components underlying BOLD in attempts to more narrowly isolate the age differences in $CMRO_2$. For instance, Ances and colleagues [226] found age differences in M, vasodilatory capacity, as the principal difference between their young and old groups. Hutchison and colleagues [10], however, isolated the differences to the decoupling change in CBF relative to $CMRO_2$, i.e. decoupling of CBF and $CMRO_2$, implicating neurovascular impairment as an underlying factor of neural efficiency [229–231]. Measuring task-induced relative changes with the calibrated approach relies on several assumptions, including a constant coupling between cerebral blood flow and cerebral blood volume across individuals and brain regions [224]. This could lead to ambiguity of interpretation as the baseline may also be changing with age. Yet the CBF–CBV coupling seems to be regionally specific, and depend on disease stages [224], therefore requiring additional physiological measures [114,148]. These factors may explain the low frequency of use of such calibrated fMRI.

(iv) General remarks on normalization and calibrating techniques

Advancing age is associated with multiple alterations in cellular and structural vasculature, leading to multiple physiological changes that directly influence the BOLD signal. However, in contrast to the over 10 000 fMRI papers on ageing during the past 20 years, there are fewer than 100 papers addressing calibration and normalization techniques of fMRI-BOLD signal, and fewer than 20 independent studies of ageing that have applied these

techniques. Future studies of ageing should consider the above correction methods, as we expand in §4.

A major issue is that nearly all the approaches reviewed above assume that vascular (age-related) factors have a linear influence on BOLD signal. However, there are nonlinear influences on the BOLD signal [145], which is rarely factored in analysis of BOLD data. Individual differences in vascular factors may occur singly, though more often in combination during ageing [22]. Moreover, these effects might be relatively independent of one another in early adulthood, but become increasingly coupled with advancing age. It is difficult to define which particular vascular factor might be primarily responsible for age-related changes and the degree and extent of their influence on BOLD signal. This is further complicated by the drugs and medication (e.g. used to normalize blood pressure) that are more often taken in old age. More research is needed to test which correction method (or combination of correction methods) can best correct for cerebrovascular influences to the BOLD signal in ageing studies.

(b) Neuronal integration

The second class of approaches focuses on estimating neuronal contributions to the BOLD signal using independent measures of neural function. The advantages of such an integration approach, as opposed to working solely with measures of neural function, are discussed below. An implicit assumption of these approaches is that they explain variability in neural activity (figure 2), but not variability related to non-neuronal physiological signals. It is also important to note that such integration will work for age effects detected jointly by both modalities, but neural signals identified uniquely by either modality may remain undetected in the data.

Electroencephalography (EEG) and MEG (together M/EEG) are two widely used non-invasive techniques in neuroscience, and ageing. Although each technique provides important insights in isolation, there are advantages to integrating fMRI and M/EEG in a multimodal approach that is more powerful than each one alone [232]. We introduced fMRI as an indirect measure of neural activity with a temporal resolution of seconds, but with a spatial resolution of millimetres. M/EEG, on the other hand, directly measure millisecond electromagnetic activity from large populations of neurons, but at the cost of far worse spatial resolution, particularly for sources of that activity that are deep in the brain. Therefore, combining evidence from M/EEG and fMRI-based techniques can to some extent complement the inherent limitations within each individual imaging modality [14,232,233]. For example, M/EEG can be used to identify neuronal components and events beyond the temporal resolution of fMRI [234,235], while fMRI can be used to improve the spatial resolution of M/EEG signals [236,237].

The primary neural source of BOLD signal is synaptic activity in the grey matter, rather than spiking activity, as indicated by a closer relationship of the BOLD signal to local field potentials than multiunit activity recordings [238–240]. BOLD–M/EEG associations span multiple frequencies, although those in the gamma band appear most notable. These gamma oscillations (greater than 30 hz) are themselves too fast for BOLD to follow, but fluctuations in their power or amplitude envelopes typically fall in similar frequency range to the BOLD signal. Nonetheless, it is important to consider all neuronal frequencies together as a collective account of the fMRI signal, even if differential contributions are found across frequencies [241–244] and even if different frequencies are differently affected by ageing.

The main advantage MEG has over EEG is that the neuronal sources, though difficult to localize precisely, are better localized than with EEG. Thus while EEG has been used to study neurocognitive ageing for many years, MEG is making an increasing contribution, particularly in combination with formal models of neuronal circuits and their dynamics [245–249]. However, reports that combine task-based MEG with task-based fMRI are only starting to emerge [245], and the combination of MEG with calibrated fMRI in cognitive experiments [250] allows integration of MEG, BOLD and CBF responses to better study differences in neurovascular coupling with ageing.

One advantage that EEG has over MEG however is that it can be acquired simultaneously with fMRI, which is especially important for task-free states that are hard to replicate when EEG and fMRI are run separately [232]. EEG has been used to separate neural from vascular components of the BOLD signal [235] and decompose subcomponents of the haemodynamic response function [192,195,251]. One challenge for concurrent EEG–fMRI remains the strong magnetic interference in EEG signals [252], although this can be mostly overcome during data processing [147]. In the context of ageing, a study using concurrent EEG–fMRI reported a small number of age-related BOLD components that were associated with EEG [253], suggesting that the combination of both methods can better dissociate neural from non-neural signals than fMRI alone. In addition, there was a set of BOLD components that were not related to EEG components, and vice versa, and it remains unknown whether these components have a neuronal or non-neuronal origin. Since MEG and EEG have different sensitivities to different types of neuronal sources (depending on the orientation and depth of the underlying synaptic currents; [254,255]), it is advantageous to combine them too [237,256]. Indeed, in future work, EEG data could be acquired simultaneously with MEG and then simultaneously with fMRI, so as to provide a bridge between all three modalities.

There are other techniques, such as measures of glucose utilization [257], beta-amyloid burden [258], synaptic density [259], optical imaging [260], PET markers of neuroinflammation [261,262], MR spectroscopic measures of the neurotransmitters [263,264] and even non-invasive brain stimulation [265,266] that may further help understand the basis of BOLD signals, but are beyond the scope of this review.

(c) fMRI modelling and signal decomposition

The third class of approaches focuses on formal modelling or statistical decomposition of the relative contribution of vascular and neuronal factors in the observed BOLD signal. Formal modelling approaches include linear models like the GLM, in which age-related variation can be captured by basis functions, as well as more complex, nonlinear, biophysical models that use differential equations that capture how neuronal events elicit variations in CBF, CBV and CVR and then ultimately changes in the BOLD signal [267,268]. Fitting these models to BOLD data results in estimates of various parameters that can then be related to age. Statistical decomposition approaches, on the other hand, are data-driven, such as principal component analysis (PCA) and

independent component analysis (ICA). Both modelling and decomposition approaches can be useful even when there are no other measures of vascular or neuronal signals (just BOLD data). However, the application and interpretation of these approaches need to be treated with care: biophysical modelling for example typically operates within a high-dimensional space with highly covarying parameters (often requiring prior constraints on the parameters, based on other physiological knowledge), while decomposition techniques will optimize the selection of signals based on a specific statistical criterion; e.g. PCA optimizes for variance, while ICA optimizes for independence.

(i) The haemodynamic response function

The temporal evolution of the BOLD response to a brief burst of neuronal activity (an impulse response) is characterized as the *haemodynamic response function* (HRF). The HRF typically peaks at 5–6 s, followed by an undershoot that lasts 20–30 s. The precise HRF shape varies across cortical regions, individuals and brain states. This variability is caused by variability in neurovascular coupling and cerebrovascular function, even in the presence of unchanged levels of neural activity [8,269]. One notable finding comes from Cohen and colleagues [53], who demonstrated that varying levels of CBF (induced by hypercapnia, normocapnia and hypocapnia) mediated the onset time, time-to-peak and amplitude of the HRF under the same visual stimulation. The HRF has also been shown to change with genetic, hormonal and other systemic fluctuations [270–272]. Regional variability in the HRF is partly dictated by the size of surrounding blood vessels, e.g. regions with larger draining veins have a more delayed HRF [273–275]. While some fMRI studies use a temporal basis set within the GLM to allow for variations in HRF shape across voxels/individuals [7,276], many use a single, 'canonical' HRF. In the latter case, any inferences about age differences in neuronal activity are complicated if there is a systematic age-related bias in the HRF [277]. For example, a 2-second mis-estimation in the latency of the HRF could (artificially) decrease the magnitude of the estimated neural response by 38% [273]. One potential way to address this would be to demonstrate the specificity of the findings to the condition of interest, but not other contrasts in the experiment.

Several studies have used multiple temporal basis functions with the GLM to capture age-related variations in the HRF shape, including approaches where estimation of the basis function parameters is jointly optimized with estimation of brain activity [278,279]. However, the results have been mixed (see [280]), which might reflect variability across studies in the tasks, the use of relatively small sample sizes and biased selection of participants (particularly when older volunteers are more healthy than average). The recent study by West *et al*. [280] addressed these problems by using a large, population-derived cohort called Cam-CAN, in which a simple sensorimotor task was optimized for detection of HRF shape [281]. This study found extensive effects of age on the HRF, particularly its latency, in many brain regions, despite the fact that there were no performance differences between young and old adults (although latencies of neuronal responses were not directly measured).

(ii) Dynamic causal modelling

Dynamic causal modelling (DCM) is a model-based approach to studying brain connectivity [282], which includes a biophysical model of the BOLD response [267,268]. DCM uses a Bayesian framework to simultaneously estimate parameters capturing neural activity (and connectivity) and parameters capturing the vascular mapping of that activity to the BOLD response. The neural activity can either be defined by experimental manipulations [282] or by assumptions about the endogenous fluctuations that occur in task-free states like rest [283]. Importantly, the simultaneous optimization of neuronal and vascular models (unlike in GLM approaches above) means that differences in the estimated vascular parameters (e.g. owing to age) are, in theory, uncontaminated by any differences in neuronal parameters. However, the model can be under-determined (more degrees of freedom in the model than in the data), requiring strong priors on some of the parameters to regularize the models [284]. These include priors based on physiological data from previous studies, or shrinkage priors that require strong evidence in order for posterior estimates to differ from their prior expectation. The model optimization is made with reference to (log)-model evidence, which accounts for both model accuracy and model complexity.

We applied DCM to resting-state data from 635 adults aged 18–88 in the CamCAN dataset [15]. A notable finding was that neural and haemodynamic parameters were independent predictors of age, supporting the hypothesis of separable mechanisms leading to age alterations in neural and vascular function. Furthermore, the neural (connectivity) parameters were related to cognitive ability, and this relationship was moderated by age, demonstrating the behavioural relevance of this approach to neurocognitive ageing. Interestingly, the same relationship to cognitive ability was not observed with traditional (correlational) analysis of BOLD functional connectivity, which confounds neural and vascular components of the BOLD signal. These findings motivate the use of modelling techniques like DCM to separate neural and vascular components of the BOLD signal.

(iii) Independent component analysis

ICA is a data-driven approach to extract signals (components) that are maximally independent across a dimension, such as across space when applied to fMRI images. McKeown and colleagues were some of the first to apply spatial ICA to fMRI BOLD data under the assumption that signal from each voxel represents a linear mixture of source signals [285]. Each ICA component consists of a spatial pattern across voxels associated with a common BOLD timecourse. These components are often dominated by neural or non-neural signals [286], and their spatial distribution (and/or power spectrum) can sometimes be used to identify vascular components (e.g. around the Circle of Willis) or other noise sources (like motion artefacts, which often appear around the edge of the brain). Another way to separate BOLD from non-BOLD components is to combine ICA with multi-echo fMRI: only ICA components dominated by BOLD signal should show a linear dependency on echo-time (TE) [287].

Most studies use ICA to extract functional networks from task-free fMRI data [15,288,289] or structured sources of signal from morphological, vascular and neuroinflammatory measures [12,262]. In task-based BOLD studies, the ICA

approach offers multiple advantages over the traditional GLM approach [290]. It can separate and remove non-neuronal signals for improving the sensitivity of subsequent task-based GLM analysis [289,291]. ICA can also identify task-based BOLD changes in a model-free manner that can minimize sensitivity to variation in the HRF shape [292,293]. Finally, ICA can dissociate between multiple concurrent processes associated with common regions under varying cognitive states [294]. Despite these advantages, future studies need to benchmark the efficiency of ICA to control for age differences in neurovascular coupling against other data-driven decomposition approaches [295] and normalization methods of task-based BOLD.

4. Towards neuro–vascular integration

The previous sections highlighted methodological approaches to addressing age-related changes in cerebrovascular function at the cellular, structural and physiological levels in the context of BOLD fMRI and neurocognitive ageing. This methodological emphasis reflects the currently dominant aim in neurocognitive ageing: to relate cognitive changes to changes in brain activity, such that changes in vascular components are confounds of no interest. Here we argue that, rather than ignoring or correcting for such confounds, we need a better understanding of the neurovascular contribution to neurocognitive ageing, and to formally integrate vascular changes into models of successful ageing.

Vascular mechanisms in the brain do not simply control blood flow to support the metabolic needs of neurons, but lead to complex neurovascular interactions that shape neuronal function in health and disease [16,25,94]. Microvascular changes lead to lacunar infarcts, cortical and subcortical microinfarcts, microbleeds and diffuse white matter disintegration, which involves myelin loss and axonal abnormalities [296]; all of which potentially impact cognition. Brain areas in relatively sparse regions of the microvascular network, including deeper structures and white matter, are particularly vulnerable, predicting specificity in resulting cognitive deficits [94]. Age-related deficits in cognitive function have been linked to cardiovascular risk factors [297], white matter hyperintensities [298], increased pulsatility [94] and neurovascular coupling impairment [16], which may act through independent pathways [299]. Furthermore, improvement in cognitive function has been linked to increase in cardiovascular health [300]. These findings suggest that the components of cerebrovascular function are not simply confounders that obscure brain–behaviour relationships, but are synergistic factors that facilitate maintenance and improvement of cognitive function across the lifespan [16,94]. Therefore, formal integration of neurovascular knowledge provides an opportunity for a more comprehensive understanding of successful cognitive function in ageing.

Current models of neurovascular ageing [25,301] provide an array of biological pathways leading to global brain tissue loss/atrophy and cognitive deficits, mainly in age-related neurodegeneration. However, such models are suboptimal for characterizing healthy and successful ageing, where cognitive function is maintained in the presence of brain atrophy [302]. In addition, the link between age-related changes in brain tissue and cognition is surprisingly weak, and it has proven difficult to establish region-by-region correlations between brain structure and cognitive function [303]. Moreover, not all cognitive abilities decline with age, nor do all older adults show cognitive decline at the same rate. Studying the effect of neurovascular ageing on brain atrophy or global cognitive decline on its own is insufficient for understanding the complex pattern of cognitive diversity and increasing individual variability in healthy ageing [304,305].

In the field of neurocognitive ageing, the advent of functional imaging and its early emphasis on functional segregation bolstered the idea that the brain can flexibly respond to age or tissue loss, by recruiting additional brain regions to support cognitive functions [306]. Many theories of cognitive ageing have since emerged [306], some proposing that the recruitment of additional brain regions improves performance, while others suggest it can impede performance [307]. Currently, there are three general models of successful ageing in terms of sustained cognitive performance: *maintenance*, *reorganization* and *reserve* [308], which are not necessarily fully compatible. In our view, these models demand more sophisticated interpretation of BOLD fMRI [309] through the integration of neurovascular ageing [12,15]. It is important to ask whether and how multiple cerebrovascular components (in models of neurovascular ageing) independently and synergistically explain multiple profiles of neural function leading to cognitive diversity in ageing [289].

We propose that one should consider cerebrovascular function as an additional predictor in the modelling of brain–behaviour relationships, rather than simply a normalization or confounding variable. This will provide a more complete interpretation of the unique and shared contributions to brain–behaviour relationships. For example, the shared variance in task performance explained by vascular and neural signals indicates the presence of a common underlying factor. Conversely, the unique variance explained by neural signals suggests that the effects are beyond differences in cerebrovascular function. Finally, unique variance explained by vascular signals may indicate that the neuronal estimates are insufficient to capture all behavioural variability and an improved definition of the neuronal estimates should be reconsidered. These scenarios are plausible in isolation or in combination with one another, but importantly their consideration provides an empirical motivation to understand what determines cognitive diversity in ageing. Furthermore, modelling and reporting the effects of cerebrovascular function on the brain–behaviour relationship is in the spirit of maximizing internal validity [310], avoiding pitfalls of modular analysis [311], transparent reporting of results, facilitation of replication and interpretation of findings within the context of the limitations of the research methodology providing the signals of interest.

In summary, we argue for the integration of neurovascular and neurocognitive research on biological, theoretical, methodological and analytical grounds. We propose that future research should focus on the interplay of vascular and neural factors for maintaining mental health across the lifespan (i.e. successful ageing) using a multi-modal, integrative approach. Integration of neurovascular and neurocognitive ageing could provide new insights into the fundamental mechanisms that regulate brain health and mental well-being. Importantly, it will determine the extent to which these factors relate to neural function, relate to

cognitive performance, and are associated with individual differences in lifestyle, demography, genetics and health. This will provide a bridge between modifiable risk and protective factors, neurovascular function and cognitive ability across the healthy adult lifespan.

5. Conclusion

With recent advances in fMRI BOLD imaging, much has been learned about the effects of age on neurovascular and neurocognitive function. It is clear that neurovascular and neuronal signals both contribute to fMRI BOLD signal, and that their interaction affects the interpretations one can draw about neurocognitive ageing. To understand the effect of ageing on brain function, a variety of techniques have been developed and validated that separate vascular from neuronal signals in BOLD-fMRI data. However, only a small fraction of fMRI studies of ageing have adopted such approaches in their analysis. We argue on biological, theoretical and analytical grounds for a better understanding of their relative contributions to fMRI. Vascular and neuronal contributions can be formally integrated in models of successful ageing, avoiding common misinterpretations of fMRI and complementing the limitations within individual modalities. Only by first understanding these mechanisms and their interactions can we subsequently address a major challenge that pervades neurovascular and neurocognitive ageing: to characterize the effects of healthy and pathological ageing at the level of vascular and neuronal network structures of the human brain across the lifespan.

Data accessibility. This article has no additional data.

Authors' contributions. K.A.T., R.N.A.H. and J.B.R. wrote the article.

Competing interests. We declare we have no competing interests.

Funding. This work is supported by the British Academy (grant no. PF160048), the Guarantors of Brain (grant no. G101149), the Wellcome Trust (grant no. 103838), the Medical Research Council (grant nos SUAG/051 G101400; and SUAG/046 G101400), European Union's Horizon 2020 (grant no. 732592) and the Cambridge NIHR Biomedical Research Centre.

Acknowledgements. We thank Wiktor Olszowy for valuable comments.

References

1. Beard JR *et al.* 2016 The World report on ageing and health: a policy framework for healthy ageing. *Lancet* **387**, 2145–2154. (doi:10.1016/S0140-6736(15)00516-4)
2. Sahakian BJ. 2014 What do experts think we should do to achieve brain health? *Neurosci. Biobehav. Rev.* **43**, 240–258. (doi:10.1016/j.neubiorev.2014.04.002)
3. Attwell D, Iadecola C. 2002 The neural basis of functional brain imaging signals. *Trends Neurosci.* **25**, 621–625. (doi:10.1016/S0166-2236(02)02264-6)
4. Hall CN, Howarth C, Kurth-Nelson Z, Mishra A. 2016 Interpreting BOLD: towards a dialogue between cognitive and cellular neuroscience. *Phil. Trans. R. Soc. B* **371**, 20150348. (doi:10.1098/rstb.2015.0348)
5. Kim S-GG, Ogawa S. 2012 Biophysical and physiological origins of blood oxygenation level-dependent fMRI signals. *J. Cereb. Blood Flow Metab.* **32**, 1188–1206. (doi:10.1038/jcbfm.2012.23)
6. Buxton RB, Uludağ K, Dubowitz DJ, Liu TT. 2004 Modeling the hemodynamic response to brain activation. *NeuroImage* **23**, S220–S233. (doi:10.1016/j.neuroimage.2004.07.013)
7. Friston KJ, Fletcher P, Josephs O, Holmes A, Rugg MD, Turner R. 1998 Event-related fMRI: characterizing differential responses. *NeuroImage* **7**, 30–40. (doi:10.1006/nimg.1997.0306)
8. Handwerker DA, Gonzalez-Castillo J, D'Esposito M, Bandettini PA. 2012 The continuing challenge of understanding and modeling hemodynamic variation in fMRI. *NeuroImage* **62**, 1017–1023. (doi:10.1016/j.neuroimage.2012.02.015)
9. Stephan KE, Weiskopf N, Drysdale PM, Robinson PA, Friston KJ. 2007 Comparing hemodynamic models with DCM. *NeuroImage* **38**, 387–401. (doi:10.1016/j.neuroimage.2007.07.040)
10. Hutchison JL, Lu H, Rypma B. 2013 Neural mechanisms of age-related slowing: the ΔCBF/$\Delta CMRO_2$ ratio mediates age-differences in BOLD signal and human performance. *Cereb. Cortex* **23**, 2337–2346. (doi:10.1093/cercor/bhs233)
11. Liu P, Hebrank AC, Rodrigue KM, Kennedy KM, Section J, Park DC, Lu H. 2013 Age-related differences in memory-encoding fMRI responses after accounting for decline in vascular reactivity. *NeuroImage* **78**, 415–425. (doi:10.1016/j.neuroimage.2013.04.053)
12. Tsvetanov KA, Henson RNA, Tyler LK, Davis SW, Shafto MA, Taylor JR, Williams N, Rowe JB. 2015 The effect of ageing on fMRI: correction for the confounding effects of vascular reactivity evaluated by joint fMRI and MEG in 335 adults. *Hum. Brain Mapp.* **36**, 2248–2269. (doi:10.1002/hbm.22768)
13. Geerligs L, Tsvetanov KA, Cam-CAN, Henson RN. 2017 Challenges in measuring individual differences in functional connectivity using fMRI: the case of healthy aging. *Hum. Brain Mapp.* **38**, 4125–4156. (doi:10.1002/hbm.23653)
14. Geerligs L, Tsvetanov KA. 2016 The use of resting state data in an integrative approach to studying neurocognitive ageing—Commentary on Campbell and Schacter (2016). *Lang. Cogn. Neurosci.* **32**, 684–691. (doi:10.1080/23273798.2016.1251600)
15. Tsvetanov KA, Henson RNA, Tyler LK, Razi A, Geerligs L, Ham TE, Rowe JB. 2016 Extrinsic and intrinsic brain network connectivity maintains cognition across the lifespan despite accelerated decay of regional brain activation. *J. Neurosci.* **36**, 3115–3126. (doi:10.1523/JNEUROSCI.2733-15.2016)
16. Abdelkarim D, Zhao Y, Turner MP, Sivakolundu DK, Lu H, Rypma B. 2019 A neural-vascular complex of age-related changes in the human brain: anatomy, physiology, and implications for neurocognitive aging. *Neurosci. Biobehav. Rev.* **107**, 927–944. (doi:10.1016/j.neubiorev.2019.09.005)
17. Dai D-F, Chen T, Johnson SC, Szeto H, Rabinovitch PS. 2012 Cardiac aging: from molecular mechanisms to significance in human health and disease. *Antioxid. Redox Signal.* **16**, 1492–1526. (doi:10.1089/ars.2011.4179)
18. Fulop GA *et al.* 2019 Role of age-related alterations of the cerebral venous circulation in the pathogenesis of vascular cognitive impairment. *Am. J. Physiol. Heart Circ. Physiol.* **316**, H1124–H1140. (doi:10.1152/ajpheart.00776.2018)
19. Paneni F, Diaz Cañestro C, Libby P, Lüscher TF, Camici GG. 2017 The aging cardiovascular system: understanding it at the cellular and clinical levels. *J. Am. Coll. Cardiol.* **69**, 1952–1967. (doi:10.1016/j.jacc.2017.01.064)
20. O'Rourke MF, Hashimoto J. 2007 Mechanical factors in arterial aging: a clinical perspective. *J. Am. Coll. Cardiol.* **50**, 1–13. (doi:10.1016/j.jacc.2006.12.050)
21. Lacolley P, Regnault V, Segers P, Laurent S. 2017 Vascular smooth muscle cells and arterial stiffening: relevance in development, aging, and disease. *Physiol. Rev.* **97**, 1555–1617. (doi:10.1152/physrev.00003.2017)
22. Kalaria RN, Hase Y. 2019 Neurovascular ageing and age-related diseases. In *Biochemistry and Cell Biology of Ageing: Part II Clinical Science*. Subcellular Biochemistry, vol. 91 (eds J Harris, V Korolchuk), pp. 477–499. Singapore, China: Springer. (doi:10.1007/978-981-13-3681-2_17)
23. Kohn JC, Lampi MC, Reinhart-King CA. 2015 Age-related vascular stiffening: causes and consequences. *Front. Genet.* **6**, 112. (doi:10.3389/FGENE.2015.00112)
24. Li Y, Choi WJ, Wei W, Song S, Zhang Q, Liu J, Wang RK. 2018 Aging-associated changes in cerebral

vasculature and blood flow as determined by quantitative optical coherence tomography angiography. *Neurobiol. Aging* **70**, 148–159. (doi:10.1016/j.neurobiolaging.2018.06.017)

25. Iadecola C. 2017 The neurovascular unit coming of age: a journey through neurovascular coupling in health and disease. *Neuron* **96**, 17–42. (doi:10.1016/j.neuron.2017.07.030)
26. Kalaria RN. 2010 Vascular basis for brain degeneration: faltering controls and risk factors for dementia. *Nutr. Rev.* **68**(Suppl 2), S74–S87. (doi:10.1111/j.1753-4887.2010.00352.x)
27. Wang JC, Bennett M. 2012 Aging and atherosclerosis: mechanisms, functional consequences, and potential therapeutics for cellular senescence. *Circ. Res.* **111**, 245–259. (doi:10.1161/CIRCRESAHA.111.261388)
28. Hall CN *et al.* 2014 Capillary pericytes regulate cerebral blood flow in health and disease. *Nature* **508**, 55–60. (doi:10.1038/nature13165)
29. Attwell D, Mishra A, Hall CN, O'Farrell FM, Dalkara T. 2016 What is a pericyte? *J. Cereb. Blood Flow Metab.* **36**, 451–455. (doi:10.1177/0271678X15610340)
30. Sweeney MD, Ayyadurai S, Zlokovic BV. 2016 Pericytes of the neurovascular unit: key functions and signaling pathways. *Nat. Neurosci.* **19**, 771–783. (doi:10.1038/nn.4288)
31. Drew PJ. 2019 Vascular and neural basis of the BOLD signal. *Curr. Opin. Neurobiol.* **58**, 61–69. (doi:10.1016/j.conb.2019.06.004)
32. Lee LM *et al.* 2019 Key aspects of neurovascular control mediated by specific populations of inhibitory cortical interneurons. *BioRxiv* 550269. (doi:10.1101/550269)
33. Uhlirova H *et al.* 2016 Cell type specificity of neurovascular coupling in cerebral cortex. *Elife* **5**, e14315. (doi:10.7554/eLife.14315)
34. Cauli B, Hamel E. 2010 Revisiting the role of neurons in neurovascular coupling. *Front. Neuroenergetics* **2**, 1–8. (doi:10.3389/fnene.2010.00009)
35. Hosford PS, Gourine AV. 2019 What is the key mediator of the neurovascular coupling response? *Neurosci. Biobehav. Rev.* **96**, 174–181. (doi:10.1016/j.neubiorev.2018.11.011)
36. Echagarruga C, Gheres K, Drew PJ. 2019 An oligarchy of NO-producing interneurons controls basal and evoked blood flow in the cortex. *bioRxiv* 555151. (doi:10.1101/555151)
37. Vazquez AL, Fukuda M, Kim SG. 2018 Inhibitory neuron activity contributions to hemodynamic responses and metabolic load examined using an inhibitory optogenetic mouse model. *Cereb. Cortex* **28**, 4105–4119. (doi:10.1093/cercor/bhy225)
38. Legon W, Punzell S, Dowlati E, Adams SE, Stiles AB, Moran RJ. 2016 Altered prefrontal excitation/inhibition balance and prefrontal output: markers of aging in human memory networks. *Cereb. Cortex* **26**, 4315–4326. (doi:10.1093/cercor/bhv200)
39. Luebke JI, Chang YM, Moore TL, Rosene DL. 2004 Normal aging results in decreased synaptic excitation and increased synaptic inhibition of layer 2/3 pyramidal cells in the monkey prefrontal cortex. *Neuroscience* **125**, 277–288. (doi:10.1016/j.neuroscience.2004.01.035)
40. McQuail JA, Frazier CJ, Bizon JL. 2015 Molecular aspects of age-related cognitive decline: the role of GABA signaling. *Trends Mol. Med.* **21**, 450–460. (doi:10.1016/j.molmed.2015.05.002)
41. Rozycka A, Liguz-Lecznar M. 2017 The space where aging acts: focus on the GABAergic synapse. *Aging Cell* **16**, 634–643. (doi:10.1111/acel.12605)
42. Sweeney MD, Zhao Z, Montagne A, Nelson AR, Zlokovic BV. 2019 Blood–brain barrier: from physiology to disease and back. *Physiol. Rev.* **99**, 21–78. (doi:10.1152/physrev.00050.2017)
43. Khakh BS, Deneen B. 2019 The emerging nature of astrocyte diversity. *Annu. Rev. Neurosci.* **42**, 187–207. (doi:10.1146/annurev-neuro-070918-050443)
44. Zonta M, Angulo MC, Gobbo S, Rosengarten B, Hossmann KA, Pozzan T, Carmignoto G. 2003 Neuron-to-astrocyte signaling is central to the dynamic control of brain microcirculation. *Nat. Neurosci.* **6**, 43–50. (doi:10.1038/nn980)
45. Petzold GC, Murthy VN. 2011 Role of astrocytes in neurovascular coupling. *Neuron* **71**, 782–797. (doi:10.1016/j.neuron.2011.08.009)
46. Cauli B, Hamel E. 2018 Brain perfusion and astrocytes. *Trends Neurosci.* **41**, 409–413. (doi:10.1016/j.tins.2018.04.010)
47. Chen BR, Kozberg MG, Bouchard MB, Shaik MA, Hillman EMC. 2014 A critical role for the vascular endothelium in functional neurovascular coupling in the brain. *J. Am. Heart Assoc.* **3**, e000787. (doi:10.1161/JAHA.114.000787)
48. Chow BW, Nuñez V, Kaplan L, Granger AJ, Bistrong K, Zucker HL, Kumar P, Sabatini BL, Gu C. 2020 Caveolae in CNS arterioles mediate neurovascular coupling. *Nature* **579**, 1–5. (doi:10.1038/s41586-020-2026-1)
49. Chen A *et al.* 2016 Frontal white matter hyperintensities, clasmatodendrosis and gliovascular abnormalities in ageing and post-stroke dementia. *Brain* **139**, 242–258. (doi:10.1093/brain/awv328)
50. Kress BT *et al.* 2014 Impairment of paravascular clearance pathways in the aging brain. *Ann. Neurol.* **76**, 845–861. (doi:10.1002/ana.24271)
51. Soreq L *et al.* 2017 Major shifts in glial regional identity are a transcriptional hallmark of human brain aging. *Cell Rep.* **18**, 557–570. (doi:10.1016/j.celrep.2016.12.011)
52. Brown GG, Eyler Zorrilla LT, Georgy B, Kindermann SS, Wong EC, Buxton RB. 2003 BOLD and perfusion response to finger–thumb apposition after acetazolamide administration: differential relationship to global perfusion. *J. Cereb. Blood Flow Metab.* **23**, 829–837. (doi:10.1097/01.WCB.0000071887.63724.B2)
53. Cohen ER, Ugurbil K, Kim S-G. 2002 Effect of basal conditions on the magnitude and dynamics of the blood oxygenation level-dependent fMRI response. *J. Cereb. Blood Flow Metab.* **22**, 1042–1053. (doi:10.1097/00004647-200209000-00002)
54. Stefanovic B, Warnking JM, Rylander KM, Pike GB. 2006 The effect of global cerebral vasodilation on focal activation hemodynamics. *NeuroImage* **30**, 726–734. (doi:10.1016/j.neuroimage.2005.10.038)
55. Takata N *et al.* 2018 Optogenetic astrocyte activation evokes BOLD fMRI response with oxygen consumption without neuronal activity modulation. *Glia* **66**, 2013–2023. (doi:10.1002/glia.23454)
56. Nagata K, Yamazaki T, Takano D, Maeda T, Fujimaki Y, Nakase T, Sato Y. 2016 Cerebral circulation in aging. *Ageing Res. Rev.* **30**, 49–60. (doi:10.1016/j.arr.2016.06.001)
57. Toth P, Tarantini S, Csiszar A, Ungvari Z. 2017 Functional vascular contributions to cognitive impairment and dementia: mechanisms and consequences of cerebral autoregulatory dysfunction, endothelial impairment, and neurovascular uncoupling in aging. *Am. J. Physiol. Heart Circ. Physiol.* **312**, H1–H20. (doi:10.1152/ajpheart.00581.2016)
58. Flück D, Beaudin AE, Steinback CD, Kumarpillai G, Shobha N, McCreary CR, Peca S, Smith EE, Poulin MJ. 2014 Effects of aging on the association between cerebrovascular responses to visual stimulation, hypercapnia and arterial stiffness. *Front. Physiol.* **5**, 1–12. (doi:10.3389/fphys.2014.00049)
59. Leenders KL *et al.* 1990 Cerebral blood flow, blood volume and oxygen utilization. Normal values and effect of age. *Brain* **113**(Pt 1), 27–47. (doi:10.1093/brain/113.1.27)
60. Reich T, Rusinek H. 1989 Cerebral cortical and white matter reactivity to carbon dioxide. *Stroke* **20**, 453–457. (doi:10.1161/01.STR.20.4.453)
61. Ambarki K, Wåhlin A, Zarrinkoob L, Wirestam R, Petr J, Malm J, Eklund A. 2015 Accuracy of parenchymal cerebral blood flow measurements using pseudocontinuous arterial spin-labeling in healthy volunteers. *AJNR. Am. J. Neuroradiol.* **36**, 1816–1821. (doi:10.3174/ajnr.A4367)
62. Tarumi T, Zhang R. 2018 Cerebral blood flow in normal aging adults: cardiovascular determinants, clinical implications, and aerobic fitness. *J. Neurochem.* **144**, 595–608. (doi:10.1111/jnc.14234)
63. Xing C-Y, Tarumi T, Liu J, Zhang Y, Turner M, Riley J, Tinajero CD, Yuan L-J, Zhang R. 2017 Distribution of cardiac output to the brain across the adult lifespan. *J. Cereb. Blood Flow Metab.* **37**, 2848–2856. (doi:10.1177/0271678X16676826)
64. Davis TL, Kwong KK, Weisskoff RM, Rosen BR. 1998 Calibrated functional MRI: mapping the dynamics of oxidative metabolism. *Proc. Natl Acad. Sci. USA* **95**, 1834–1839. (doi:10.1073/pnas.95.4.1834)
65. Hoge RD, Atkinson J, Gill B, Crelier GR, Marrett S, Pike GB. 1999 Linear coupling between cerebral blood flow and oxygen consumption in activated human cortex. *Proc. Natl Acad. Sci. USA* **96**, 9403–9408. (doi:10.1073/pnas.96.16.9403)
66. Hoge RD, Atkinson J, Gill B, Crelier GR, Marrett S, Pike GB. 1999 Investigation of BOLD signal dependence on cerebral blood flow and oxygen consumption: the deoxyhemoglobin dilution model. *Magn. Reson. Med.* **42**, 849–863. (doi:10.1002/

(SICI)1522-2594(199911)42:5<849::AID-MRM4>3.0.CO;2-Z)

67. Ainslie PN, Ashmead JC, Ide K, Morgan BJ, Poulin MJ. 2005 Differential responses to CO_2 and sympathetic stimulation in the cerebral and femoral circulations in humans. *J. Physiol.* **566**, 613–624. (doi:10.1113/jphysiol.2005.087320)
68. Jensen KE, Thomsen C, Henriksen O. 1988 *In vivo* measurement of intracellular pH in human brain during different tensions of carbon dioxide in arterial blood. A 31P-NMR study. *Acta Physiol. Scand.* **134**, 295–298. (doi:10.1111/j.1748-1716.1988.tb08492.x)
69. Lambertsen CJ, Semple SJG, Smyth MG, Gelfand R. 1961 H^+ and pCO_2 as chemical factors in respiratory and cerebral circulatory control. *J. Appl. Physiol.* **16**, 473–484. (doi:10.1152/jappl.1961.16.3.473)
70. Lassen NA. 1968 Brain extracellular pH: the main factor controlling cerebral blood flow. *Scand. J. Clin. Lab. Invest.* **22**, 247–251. (doi:10.3109/00365516809167060)
71. Ainslie PN, Duffin J. 2009 Integration of cerebrovascular CO_2 reactivity and chemoreflex control of breathing: mechanisms of regulation, measurement, and interpretation. *Am. J. Physiol. Regul. Integr. Comp. Physiol.* **296**, 1473–1495. (doi:10.1152/ajpregu.91008.2008)
72. Ito H, Takahashi K, Hatazawa J, Kim SG, Kanno I. 2001 Changes in human regional cerebral blood flow and cerebral blood volume during visual stimulation measured by positron emission tomography. *J. Cereb. Blood Flow Metab.* **21**, 608–612. (doi:10.1097/00004647-200105000-00015)
73. Chen A, Shyr MH, Chen TY, Lai HY, Lin CC, Yen PS. 2006 Dynamic CT perfusion imaging with acetazolamide challenge for evaluation of patients with unilateral cerebrovascular steno-occlusive disease. *Am. J. Neuroradiol.* **27**, 1876–1881.
74. Willie CK, Tzeng Y-C, Fisher JA, Ainslie PN. 2014 Integrative regulation of human brain blood flow. *J. Physiol.* **592**, 841–859. (doi:10.1113/jphysiol.2013.268953)
75. Rostrup E, Larsson HBW, Toft PB, Garde K, Ring PB, Henriksen O. 1996 Susceptibility contrast imaging of CO_2-induced changes in the blood volume of the human brain. *Acta Radiol.* **37**, 813–822. (doi:10.1177/02841851960373P276)
76. Rostrup E, Larsson HBW, Toft PB, Garde K, Thomsen C, Ring P, Søndergaard L, Henriksen O. 1994 Functional MRI of CO_2 induced increase in cerebral perfusion. *NMR Biomed.* **7**, 29–34. (doi:10.1002/nbm.1940070106)
77. Keyeux A, Ochrymowicz-Bemelmans D, Charlier AA. 1995 Induced response to hypercapnia in the two-compartment total cerebral blood volume: influence on brain vascular reserve and flow efficiency. *J. Cereb. Blood Flow Metab.* **15**, 1121–1131. (doi:10.1038/jcbfm.1995.139)
78. Wagerle LC, Mishra OP. 1988 Mechanism of CO_2 response in cerebral arteries of the newborn pig: role of phospholipase, cyclooxygenase, and lipoxygenase pathways. *Circ. Res.* **62**, 1019–1026. (doi:10.1161/01.RES.62.5.1019)
79. Tsuda Y, Hartmann A. 1989 Changes in hyperfrontality of cerebral blood flow and carbon dioxide reactivity with age. *Stroke* **20**, 1667–1673. (doi:10.1161/01.STR.20.12.1667)
80. Yamaguchi F, Meyer JS, Sakai F, Yamamoto M. 1979 Normal human aging and cerebral vasoconstrictive responses to hypocapnia. *J. Neurol. Sci.* **44**, 87–94. (doi:10.1016/0022-510X(79)90226-0)
81. Geurts LJ, Bhogal AA, Siero JCW, Luijten PR, Biessels GJ, Zwanenburg JJM. 2018 Vascular reactivity in small cerebral perforating arteries with 7 T phase contrast MRI—a proof of concept study. *NeuroImage* **172**, 470–477. (doi:10.1016/j.neuroimage.2018.01.055)
82. Ito H, Kanno I, Ibaraki M, Hatazawa J. 2002 Effect of aging on cerebral vascular response to $Paco_2$ changes in humans as measured by positron emission tomography. *J. Cereb. Blood Flow Metab.* **22**, 997–1003. (doi:10.1097/00004647-200208000-00011)
83. Fang HCH. 1976 Observations on aging characteristics of cerebral blood vessels, macroscopic and microscopic features. *Neurobiol. Aging* **3**, 155–167.
84. Brandes RP, Fleming I, Busse R. 2005 Endothelial aging. *Cardiovasc. Res.* **66**, 286–294. (doi:10.1016/j.cardiores.2004.12.027)
85. Hatazawa J, Shimosegawa E, Satoh T, Toyoshima H, Okudera T. 1997 Subcortical hypoperfusion associated with asymptomatic white matter lesions on magnetic resonance imaging. *Stroke* **28**, 1944–1947. (doi:10.1161/01.STR.28.10.1944)
86. Kuwabara Y, Ichiya Y, Sasaki M, Yoshida T, Fukumura T, Masuda K, Ibayashi S, Fujishima M. 1996 Cerebral blood flow and vascular response to hypercapnia in hypertensive patients with leukoaraiosis. *Ann. Nucl. Med.* **10**, 293–298. (doi:10.1007/BF03164735)
87. Mandeville JB, Marota JJA, Ayata C, Zaharchuk G, Moskowitz MA, Rosen BR, Weisskoff RM. 1999 Evidence of a cerebrovascular postarteriole windkessel with delayed compliance. *J. Cereb. Blood Flow Metab.* **19**, 679–689. (doi:10.1097/00004647-199906000-00012)
88. Wagshul ME, Eide PK, Madsen JR. 2011 The pulsating brain: a review of experimental and clinical studies of intracranial pulsatility. *Fluids Barriers CNS* **8**, 5. (doi:10.1186/2045-8118-8-5)
89. Vlachopoulos C, O'Rourke M, Nichols WW, O'Rourke M, Nichols WW. 2011 *McDonald's blood flow in arteries 6th edition: theoretical, experimental and clinical principles*. Boca Raton, FL: CRC Press.
90. Mitchell GF *et al.* 2011 Arterial stiffness, pressure and flow pulsatility and brain structure and function: the Age, Gene/Environment Susceptibility—Reykjavik Study. *Brain* **134**, 3398–3407. (doi:10.1093/brain/awr253)
91. Tarumi T, Ayaz Khan M, Liu J, Tseng BM, Parker R, Riley J, Tinajero C, Zhang R. 2014 Cerebral hemodynamics in normal aging: central artery stiffness, wave reflection, and pressure pulsatility. *J. Cereb. Blood Flow Metab.* **34**, 971–978. (doi:10.1038/jcbfm.2014.44)
92. Mok V *et al.* 2012 Transcranial Doppler ultrasound for screening cerebral small vessel disease: a community study. *Stroke* **43**, 2791–2793. (doi:10.1161/STROKEAHA.112.665711)
93. Webb AJS, Simoni M, Mazzucco S, Kuker W, Schulz U, Rothwell PM. 2012 Increased cerebral arterial pulsatility in patients with leukoaraiosis. *Stroke* **43**, 2631–2636. (doi:10.1161/STROKEAHA.112.655837)
94. Wåhlin A, Nyberg L. 2019 At the heart of cognitive functioning in aging. *Trends Cogn. Sci.* **23**, 717–720. (doi:10.1016/j.tics.2019.06.004)
95. Dagli MS, Ingeholm JE, Haxby JV. 1999 Localization of cardiac-induced signal change in fMRI. *NeuroImage* **9**, 407–415. (doi:10.1006/nimg.1998.0424)
96. Makedonov I, Chen JJ, Masellis M, MacIntosh BJ. 2016 Physiological fluctuations in white matter are increased in Alzheimer's disease and correlate with neuroimaging and cognitive biomarkers. *Neurobiol. Aging* **37**, 12–18. (doi:10.1016/j.neurobiolaging.2015.09.010)
97. Makedonov I, Black SE, Macintosh BJ. 2013 BOLD fMRI in the white matter as a marker of aging and small vessel disease. *PLoS ONE* **8**, e67652. (doi:10.1371/journal.pone.0067652)
98. Theyers AE, Goldstein BI, Metcalfe AW, Robertson AD, MacIntosh BJ. 2018 Cerebrovascular blood oxygenation level dependent pulsatility at baseline and following acute exercise among healthy adolescents. *J. Cereb. Blood Flow Metab.* **39**, 1737–1749. (doi:10.1177/0271678X18766771)
99. Viessmann O, Möller HE, Jezzard P. 2019 Dual regression physiological modeling of resting-state EPI power spectra: effects of healthy aging. *NeuroImage* **187**, 68–76. (doi:10.1016/j.neuroimage.2018.01.011)
100. Viessmann O, Möller HE, Jezzard P. 2017 Cardiac cycle-induced EPI time series fluctuations in the brain: their temporal shifts, inflow effects and T_2^* fluctuations. *NeuroImage* **162**, 93–105. (doi:10.1016/j.neuroimage.2017.08.061)
101. Battisti-Charbonney A, Fisher J, Duffin J. 2011 The cerebrovascular response to carbon dioxide in humans. *J. Physiol.* **589**, 3039–3048. (doi:10.1113/jphysiol.2011.206052)
102. Jeong S-M, Kim S-O, DeLorey DS, Babb TG, Levine BD, Zhang R. 2016 Lack of correlation between cerebral vasomotor reactivity and dynamic cerebral autoregulation during stepwise increases in inspired CO_2 concentration. *J. Appl. Physiol.* **120**, 1434–1441. (doi:10.1152/japplphysiol.00390.2015)
103. Joutel A *et al.* 2010 Cerebrovascular dysfunction and microcirculation rarefaction precede white matter lesions in a mouse genetic model of cerebral ischemic small vessel disease. *J. Clin. Invest.* **120**, 433–445. (doi:10.1172/JCI39733)
104. Purkayastha S *et al.* 2014 Impaired cerebrovascular hemodynamics are associated with cerebral white matter damage. *J. Cereb. Blood Flow Metab.* **34**, 228–234. (doi:10.1038/jcbfm.2013.180)

105. Iannetti GD, Wise RG. 2007 BOLD functional MRI in disease and pharmacological studies: room for improvement? *Magn. Reson. Imaging* **25**, 978–988. (doi:10.1016/j.mri.2007.03.018)
106. Mintun MA, Raichle ME, Martin WR, Herscovitch P. 1984 Brain oxygen utilization measured with O-15 radiotracers and positron emission tomography. *J. Nucl. Med.* **25**, 177–187.
107. Østergaard L. 2005 Principles of cerebral perfusion imaging by bolus tracking. *J. Magn. Reson. Imaging* **22**, 710–717. (doi:10.1002/jmri.20460)
108. Belliveau JW, Kennedy DN, McKinstry RC, Buchbinder BR, Weisskoff RM, Cohen MS, Vevea JM, Brady TJ, Rosen BR. 1991 Functional mapping of the human visual cortex by magnetic resonance imaging. *Science* **254**, 716–719. (doi:10.1126/science.1948051)
109. Detre Ja, Wang J, Wang Z, Rao H. 2009 Arterial spin-labeled perfusion MRI in basic and clinical neuroscience. *Curr. Opin. Neurol.* **22**, 348–355. (doi:10.1097/WCO.0b013e32832d9505)
110. Chen JJ, Wieckowska M, Meyer E, Pike GB. 2008 Cerebral blood flow measurement using fMRI and PET: a cross-validation study. *Int. J. Biomed. Imaging* **2008**, 516359. (doi:10.1155/2008/516359)
111. Detre JA, Subramanian VH, Mitchell MD, Smith DS, Kobayashi A, Zaman A, Leigh JS. 1990 Measurement of regional cerebral blood flow in cat brain using intracarotid $^{2}H_2O$ and ^{2}H NMR imaging. *Magn. Reson. Med.* **14**, 389–395. (doi:10.1002/mrm.1910140223)
112. Eleff SM, Schnall MD, Ligetti L, Osbakken M, Subramanian H, Chance B, Leigh JS. 1988 Concurrent measurements of cerebral blood flow, sodium, lactate, and high-energy phosphate metabolism using ^{19}F, ^{23}Na, ^{1}H, and ^{31}P nuclear magnetic resonance spectroscopy. *Magn. Reson. Med.* **7**, 412–424. (doi:10.1002/mrm.1910070404)
113. Heijtel DFR *et al.* 2014 Accuracy and precision of pseudo-continuous arterial spin labeling perfusion during baseline and hypercapnia: a head-to-head comparison with ^{15}O H_2O positron emission tomography. *NeuroImage* **92**, 182–192. (doi:10.1016/j.neuroimage.2014.02.011)
114. Hua J, Liu P, Kim T, Donahue M, Rane S, Chen JJ, Qin Q, Kim S-G. 2019 MRI techniques to measure arterial and venous cerebral blood volume. *NeuroImage* **187**, 17–31. (doi:10.1016/j.neuroimage.2018.02.027)
115. Pekar J, Ligeti L, Ruttner Z, Lyon RC, Sinnwell TM, van Gelderen P, Fiat D, Moonen CT, McLaughlin AC. 1991 *In vivo* measurement of cerebral oxygen consumption and blood flow using ^{17}O magnetic resonance imaging. *Magn. Reson. Med.* **21**, 313–319. (doi:10.1002/mrm.1910210217)
116. Alsop DC *et al.* 2015 Recommended implementation of arterial spin-labeled perfusion MRI for clinical applications: a consensus of the ISMRM perfusion study group and the European consortium for ASL in dementia. *Magn. Reson. Med.* **73**, 102–116. (doi:10.1002/mrm.25197)
117. Leoni RF, Oliveira IAF, Pontes-Neto OM, Santos AC, Leite JP. 2017 Cerebral blood flow and vasoreactivity in aging: an arterial spin labeling study. *Braz. J. Med. Biol. Res.* **50**, e5670. (doi:10.1590/1414-431x20175670)
118. Tsvetanov KA, Henson RNA, Jones PS, Mutsaerts H-J, Fuhrmann D, Tyler LK, Cam-CAN, Rowe JB. 2020 The effects of age on resting-state BOLD signal variability is explained by cardiovascular and cerebrovascular factors. *Psychophysiology* **00**, e13714. (doi:10.1111/psyp.13714)
119. Zhang N, Gordon ML, Goldberg TE. 2017 Cerebral blood flow measured by arterial spin labeling MRI at resting state in normal aging and Alzheimer's disease. *Neurosci. Biobehav. Rev.* **72**, 168–175. (doi:10.1016/j.neubiorev.2016.11.023)
120. Biagi L, Abbruzzese A, Bianchi MC, Alsop DC, Del Guerra A, Tosetti M. 2007 Age dependence of cerebral perfusion assessed by magnetic resonance continuous arterial spin labeling. *J. Magn. Reson. Imaging* **25**, 696–702. (doi:10.1002/jmri.20839)
121. Preibisch C *et al.* 2011 Age-related cerebral perfusion changes in the parietal and temporal lobes measured by pulsed arterial spin labeling. *J. Magn. Reson. Imaging* **34**, 1295–1302. (doi:10.1002/jmri.22788)
122. Salat DH, Lee SY, van der Kouwe aJ, Greve DN, Fischl B, Rosas HD. 2009 Age-associated alterations in cortical gray and white matter signal intensity and gray to white matter contrast. *NeuroImage* **48**, 21–28. (doi:10.1016/j.neuroimage.2009.06.074)
123. Detre JA, Rao H, Wang DJ, Chen YF, Wang Z. 2012 Applications of arterial spin labeled MRI in the brain. *J. Magn. Reson. Imaging* **35**, 1026–1037. (doi:10.1002/jmri.23581)
124. Mutsaerts HJ, Petr J, Václavů L, van Dalen JW, Robertson AD, Caan MW, Masellis M, Nederveen AJ, Richard E, MacIntosh BJ. 2017 The spatial coefficient of variation in arterial spin labeling cerebral blood flow images. *J. Cereb. Blood Flow Metab.* **37**, 3184–3192. (doi:10.1177/0271678X16683690)
125. Dai W, Fong T, Jones RN, Marcantonio E, Schmitt E, Inouye SK, Alsop DC. 2017 Effects of arterial transit delay on cerebral blood flow quantification using arterial spin labeling in an elderly cohort. *J. Magn. Reson. Imaging* **45**, 472–481. (doi:10.1002/jmri.25367)
126. Bangen KJ *et al.* 2014 Interactive effects of vascular risk burden and advanced age on cerebral blood flow. *Front. Aging Neurosci.* **6**, 1–10. (doi:10.3389/fnagi.2014.00159)
127. Ighodaro ET *et al.* 2017 Risk factors and global cognitive status related to brain arteriolosclerosis in elderly individuals. *J. Cereb. Blood Flow Metab.* **37**, 201–216. (doi:10.1177/0271678X15621574)
128. Hirao K, Ohnishi T, Matsuda H, Nemoto K, Hirata Y, Yamashita F, Asada T, Iwamoto T. 2006 Functional interactions between entorhinal cortex and posterior cingulate cortex at the very early stage of Alzheimer's disease using brain perfusion single-photon emission computed tomography. *Nucl. Med. Commun.* **27**, 151–156. (doi:10.1097/01.mnm.0000189783.39411.ef)
129. Matsuda H, Kitayama N, Ohnishi T, Asada T, Nakano S, Sakamoto S, Imabayashi E, Katoh A. 2002 Longitudinal evaluation of both morphologic and functional changes in the same individuals with Alzheimer's disease. *J. Nucl. Med.* **43**, 304–311.
130. Ruitenberg A, den Heijer T, Bakker SLM, van Swieten JC, Koudstaal PJ, Hofman A, Breteler MMB. 2005 Cerebral hypoperfusion and clinical onset of dementia: the Rotterdam study. *Ann. Neurol.* **57**, 789–794. (doi:10.1002/ana.20493)
131. Grade M, Hernandez Tamames JA, Pizzini FB, Achten E, Golay X, Smits M. 2015 A neuroradiologist's guide to arterial spin labeling MRI in clinical practice. *Neuroradiology* **57**, 1181–1202. (doi:10.1007/s00234-015-1571-z)
132. Clement P *et al.* 2018 Variability of physiological brain perfusion in healthy subjects—a systematic review of modifiers. Considerations for multi-center ASL studies. *J. Cereb. Blood Flow Metab.* **38**, 1418–1437. (doi:10.1177/0271678X17702156)
133. Addicott MA *et al.* 2009 The effect of daily caffeine use on cerebral blood flow: how much caffeine can we tolerate? *Hum. Brain Mapp.* **30**, 3102–3114. (doi:10.1002/hbm.20732)
134. Domino EF, Ni L, Xu Y, Koeppe RA, Guthrie S, Zubieta JK. 2004 Regional cerebral blood flow and plasma nicotine after smoking tobacco cigarettes. *Prog. Neuropsychopharmacol. Biol. Psychiatry* **28**, 319–327. (doi:10.1016/j.pnpbp.2003.10.011)
135. MacIntosh BJ, Crane DE, Sage MD, Rajab AS, Donahue MJ, McIlroy WE, Middleton LE. 2014 Impact of a single bout of aerobic exercise on regional brain perfusion and activation responses in healthy young adults. *PLoS ONE* **9**, e8513. (doi:10.1371/journal.pone.0085163)
136. Merola A *et al.* 2017 Mapping the pharmacological modulation of brain oxygen metabolism: the effects of caffeine on absolute $CMRO_2$ measured using dual calibrated fMRI. *NeuroImage* **155**, 331–343. (doi:10.1016/j.neuroimage.2017.03.028)
137. Macoveanu J, Rowe JB, Hornboll B, Elliott R, Paulson OB, Knudsen GM, Siebner HR. 2013 Serotonin 2A receptors contribute to the regulation of risk-averse decisions. *NeuroImage* **83**, 35–44. (doi:10.1016/j.neuroimage.2013.06.063)
138. Rae CL *et al.* 2016 Atomoxetine restores the response inhibition network in Parkinson's disease. *Brain* **139**, 2235–2248. (doi:10.1093/brain/aww138)
139. Zebrowitz L, Ward N, Boshyan J, Gutchess A, Hadjikhani N. 2016 Dedifferentiated face processing in older adults is linked to lower resting state metabolic activity in fusiform face area. *Brain Res.* **1644**, 22–31. (doi:10.1016/j.brainres.2016.05.007)
140. Liu P, De Vis JB, Lu H. 2019 Cerebrovascular reactivity (CVR) MRI with CO_2 challenge: a technical review. *NeuroImage* **187**, 104–115. (doi:10.1016/j.neuroimage.2018.03.047)
141. Bandettini Pa, Wong EC. 1997 A hypercapnia-based normalization method for improved spatial localization of human brain activation with fMRI. *NMR Biomed.* **10**, 197–203. (doi:10.1002/

(SICI)1099-1492(199706/08)10:4/5<197::AID-NBM466>3.0.CO;2-S)

142. Liau J, Liu TT. 2009 Inter-subject variability in hypercapnic normalization of the BOLD fMRI response. *NeuroImage* **45**, 420–430. (doi:10.1016/j.neuroimage.2008.11.032)
143. Halani S, Kwinta JB, Golestani AM, Khatamian YB, Chen JJ. 2015 Comparing cerebrovascular reactivity measured using BOLD and cerebral blood flow MRI: the effect of basal vascular tension on vasodilatory and vasoconstrictive reactivity. *NeuroImage* **110**, 110–123. (doi:10.1016/j.neuroimage.2015.01.050)
144. Hoge RD, Atkinson J, Gill B, Crelier GR, Marrett S, Pike GB. 1999 Stimulus-dependent BOLD and perfusion dynamics in human V1. *NeuroImage* **9**, 573–585. (doi:10.1006/nimg.1999.0443)
145. Mitsis GD, Ainslie PN, Poulin MJ, Robbins PA, Marmarelis VZ. 2004 Nonlinear modeling of the dynamic effects of arterial pressure and blood gas variations on cerebral blood flow in healthy humans. *Adv. Exp. Med. Biol.* **551**, 259–265. (doi:10.1007/0-387-27023-X_39)
146. Sobczyk O, Battisti-Charbonney a, Fierstra J, Mandell DM, Poublanc J, Crawley AP, Mikulis DJ, Duffin J, Fisher JA. 2014 A conceptual model for CO_2-induced redistribution of cerebral blood flow with experimental confirmation using BOLD MRI. *NeuroImage* **92C**, 56–68. (doi:10.1016/j.neuroimage.2014.01.051)
147. Liu Z, de Zwart JA, van Gelderen P, Kuo L-W, Duyn JH. 2012 Statistical feature extraction for artifact removal from concurrent fMRI-EEG recordings. *NeuroImage* **59**, 2073–2087. (doi:10.1016/j.neuroimage.2011.10.042)
148. Germuska M, Wise RG. 2019 Calibrated fMRI for mapping absolute $CMRO_2$: practicalities and prospects. *NeuroImage* **187**, 145–153. (doi:10.1016/j.neuroimage.2018.03.068)
149. Lu H, Liu P, Yezhuvath U, Cheng Y, Marshall O, Ge Y. 2014 MRI mapping of cerebrovascular reactivity via gas inhalation challenges. *J. Vis. Exp.* **94**, e52306. (doi:10.3791/52306)
150. Rostrup E, Law I, Blinkenberg M, Larsson HBW, Born AP, Holm S, Paulson OB. 2000 Regional differences in the CBF and BOLD responses to hypercapnia: a combined PET and fMRI study. *NeuroImage* **11**, 87–97. (doi:10.1006/nimg.1999.0526)
151. Hare HV, Germuska M, Kelly ME, Bulte DP. 2013 Comparison of CO_2 in air versus carbogen for the measurement of cerebrovascular reactivity with magnetic resonance imaging. *J. Cereb. Blood Flow Metab.* **33**, 1799–1805. (doi:10.1038/jcbfm.2013.131)
152. Zhou Y, Rodgers ZB, Kuo AH. 2015 Cerebrovascular reactivity measured with arterial spin labeling and blood oxygen level dependent techniques. *Magn. Reson. Imaging* **33**, 566–576. (doi:10.1016/j.mri.2015.02.018)
153. Kassner A, Winter JD, Poublanc J, Mikulis DJ, Crawley AP. 2010 Blood-oxygen level dependent MRI measures of cerebrovascular reactivity using a controlled respiratory challenge: reproducibility and gender differences. *J. Magn. Reson. Imaging* **31**, 298–304. (doi:10.1002/jmri.22044)
154. Cohen ER, Rostrup E, Sidaros K, Lund TE, Paulson OB, Ugurbil K, Kim S-G. 2004 Hypercapnic normalization of BOLD fMRI: comparison across field strengths and pulse sequences. *NeuroImage* **23**, 613–624. (doi:10.1016/j.neuroimage.2004.06.021)
155. De Vis JB, Hendrikse J, Bhogal A, Adams A, Kappelle LJ, Petersen ET. 2015 Age-related changes in brain hemodynamics; a calibrated MRI study. *Hum. Brain Mapp.* **36**, 3973–3987. (doi:10.1002/hbm.22891)
156. Lu H, Xu F, Rodrigue KM, Kennedy KM, Cheng Y, Flicker B, Hebrank AC, Uh J, Park DC. 2011 Alterations in cerebral metabolic rate and blood supply across the adult lifespan. *Cereb. Cortex* **21**, 1426–1434. (doi:10.1093/cercor/bhq224)
157. Thomas BP, Liu P, Park DC, van Osch MJP, Lu H. 2014 Cerebrovascular reactivity in the brain white matter: magnitude, temporal characteristics, and age effects. *J. Cereb. Blood Flow Metab.* **34**, 242–247. (doi:10.1038/jcbfm.2013.194)
158. Gauthier CJ, Madjar C, Desjardins-Crépeau L, Bellec P, Bherer L, Hoge RD. 2013 Age dependence of hemodynamic response characteristics in human functional magnetic resonance imaging. *Neurobiol. Aging* **34**, 1469–1485. (doi:10.1016/j.neurobiolaging.2012.11.002)
159. Song Z, McDonough IM, Liu P, Lu H, Park DC. 2016 Cortical amyloid burden and age moderate hippocampal activity in cognitively-normal adults. *NeuroImage Clin.* **12**, 78–84. (doi:10.1016/j.nicl.2016.05.013)
160. Liu P, Glover GH, Mueller BA, Greve DN, Brown GG. 2012 An introduction to normalization and calibration methods in functional MRI. *Psychometrika* **78**, 308–321. (doi:10.1007/s11336-012-9309-x)
161. Spano VR *et al.* 2013 CO_2 blood oxygen level-dependent MR mapping of cerebrovascular reserve in a clinical population: safety, tolerability, and technical feasibility. *Radiology* **266**, 592–598. (doi:10.1148/radiol.12112795)
162. Driver ID, Whittaker JR, Bright MG, Muthukumaraswamy SD, Murphy K. 2016 Arterial CO_2 fluctuations modulate neuronal rhythmicity: implications for MEG and fMRI studies of resting-state networks. *J. Neurosci.* **36**, 8541–8550. (doi:10.1523/JNEUROSCI.4263-15.2016)
163. Golestani AM, Kwinta JB, Strother SC, Khatamian YB, Chen JJ. 2016 The association between cerebrovascular reactivity and resting-state fMRI functional connectivity in healthy adults: the influence of basal carbon dioxide. *NeuroImage* **132**, 301–313. (doi:10.1016/j.neuroimage.2016.02.051)
164. Marshall O, Uh J, Lurie D, Lu H, Milham MP, Ge Y. 2015 The influence of mild carbon dioxide on brain functional homotopy using resting-state fMRI. *Hum. Brain Mapp.* **36**, 3912–3921. (doi:10.1002/hbm.22886)
165. Xu F, Uh J, Brier MR, Hart J, Yezhuvath US, Gu H, Yang Y, Lu H. 2011 The influence of carbon dioxide on brain activity and metabolism in conscious humans. *J. Cereb. Blood Flow Metab.* **31**, 58–67. (doi:10.1038/jcbfm.2010.153)
166. Hall EL, Driver ID, Croal PL, Francis ST, Gowland PA, Morris PG, Brookes MJ. 2011 The effect of hypercapnia on resting and stimulus induced MEG signals. *NeuroImage* **58**, 1034–1043. (doi:10.1016/j.neuroimage.2011.06.073)
167. Liu P, Welch BG, Li Y, Gu H, King D, Yang Y, Pinho M, Lu H. 2017 Multiparametric imaging of brain hemodynamics and function using gas-inhalation MRI. *NeuroImage* **146**, 715–723. (doi:10.1016/j.neuroimage.2016.09.063)
168. Kastrup A, Krüger G, Glover GH, Moseley ME. 1999 Assessment of cerebral oxidative metabolism with breath holding and fMRI. *Magn. Reson. Med.* **42**, 608–611. (doi:10.1002/(SICI)1522-2594(199909)42:3<608::AID-MRM26>3.0.CO;2-I)
169. Urback AL, MacIntosh BJ, Goldstein BI. 2017 Cerebrovascular reactivity measured by functional magnetic resonance imaging during breath-hold challenge: a systematic review. *Neurosci. Biobehav. Rev.* **79**, 27–47. (doi:10.1016/j.neubiorev.2017.05.003)
170. Bulte DP, Drescher K, Jezzard P. 2009 Comparison of hypercapnia-based calibration techniques for measurement of cerebral oxygen metabolism with MRI. *Magn. Reson. Med.* **61**, 391–398. (doi:10.1002/mrm.21862)
171. Fukunaga M, Horovitz SG, de Zwart JA, van Gelderen P, Balkin TJ, Braun AR, Duyn JH. 2008 Metabolic origin of BOLD signal fluctuations in the absence of stimuli. *J. Cereb. Blood Flow Metab.* **28**, 1377–1387. (doi:10.1038/jcbfm.2008.25)
172. Handwerker Da, Gazzaley A, Inglis Ba, D'Esposito M. 2007 Reducing vascular variability of fMRI data across aging populations using a breathholding task. *Hum. Brain Mapp.* **28**, 846–859. (doi:10.1002/hbm.20307)
173. Kastrup A, Krüger G, Neumann-Haefelin T, Moseley ME. 2001 Assessment of cerebrovascular reactivity with functional magnetic resonance imaging: comparison of CO_2 and breath holding. *Magn. Reson. Imaging* **19**, 13–20. (doi:10.1016/S0730-725X(01)00227-2)
174. Murphy K, Harris AD, Wise RG. 2011 Robustly measuring vascular reactivity differences with breath-hold: normalising stimulus-evoked and resting state BOLD fMRI data. *NeuroImage* **54**, 369–379. (doi:10.1016/j.neuroimage.2010.07.059)
175. Tancredi FB, Hoge RD. 2013 Comparison of cerebral vascular reactivity measures obtained using breath-holding and CO_2 inhalation. *J. Cereb. Blood Flow Metab.* **33**, 1066–1074. (doi:10.1038/jcbfm.2013.48)
176. Bright MG, Murphy K. 2013 Reliable quantification of BOLD fMRI cerebrovascular reactivity despite poor breath-hold performance. *NeuroImage* **83**, 559–568. (doi:10.1016/j.neuroimage.2013.07.007)
177. Lipp I, Murphy K, Caseras X, Wise RG. 2015 Agreement and repeatability of vascular reactivity estimates based on a breath-hold task and a resting state scan. *NeuroImage* **113**, 387–396. (doi:10.1016/j.neuroimage.2015.03.004)

178. Bright MG, Bulte DP, Jezzard P, Duyn JH. 2009 Characterization of regional heterogeneity in cerebrovascular reactivity dynamics using novel hypocapnia task and BOLD fMRI. *NeuroImage* **48**, 166–175. (doi:10.1016/j.neuroimage.2009.05.026)
179. Magon S, Basso G, Farace P, Ricciardi GK, Beltramello A, Sbarbati A. 2009 Reproducibility of BOLD signal change induced by breath holding. *NeuroImage* **45**, 702–712. (doi:10.1016/j.neuroimage.2008.12.059)
180. Scouten A, Schwarzbauer C. 2008 Paced respiration with end-expiration technique offers superior BOLD signal repeatability for breath-hold studies. *NeuroImage* **43**, 250–257. (doi:10.1016/j.neuroimage.2008.03.052)
181. Thomason ME, Glover GH. 2008 Controlled inspiration depth reduces variance in breath-holding-induced BOLD signal. *NeuroImage* **39**, 206–214. (doi:10.1016/j.neuroimage.2007.08.014)
182. Pinto J, Jorge J, Sousa I, Vilela P, Figueiredo P. 2016 Fourier modeling of the BOLD response to a breath-hold task: optimization and reproducibility. *NeuroImage* **135**, 223–231. (doi:10.1016/j.neuroimage.2016.02.037)
183. van Niftrik CHB, Piccirelli M, Bozinov O, Pangalu A, Valavanis A, Regli L, Fierstra J. 2016 Fine tuning breath-hold-based cerebrovascular reactivity analysis models. *Brain Behav.* **6**, 1–13. (doi:10.1002/brb3.380)
184. Chang C, Thomason ME, Glover GH. 2008 Mapping and correction of vascular hemodynamic latency in the BOLD signal. *NeuroImage* **43**, 90–102. (doi:10.1016/j.neuroimage.2008.06.030)
185. Di X, Kannurpatti SS, Rypma B, Biswal BB. 2012 Calibrating BOLD fMRI activations with neurovascular and anatomical constraints. *Cereb. Cortex* **1817**, 1–9. (doi:10.1093/cercor/bhs001)
186. Kannurpatti SS, Motes MA, Rypma B, Biswal BB. 2011 Non-neural BOLD variability in block and event-related paradigms. *Magn. Reson. Imaging* **29**, 140–146. (doi:10.1016/j.mri.2010.07.006)
187. Thomason ME, Foland LC, Glover GH. 2007 Calibration of BOLD fMRI using breath holding reduces group variance during a cognitive task. *Hum. Brain Mapp.* **28**, 59–68. (doi:10.1002/hbm.20241)
188. Di Luft CB, Baker R, Goldstone A, Zhang Y, Kourtzi Z. 2016 Learning temporal statistics for sensory predictions in aging. *J. Cogn. Neurosci.* **28**, 418–432. (doi:10.1162/jocn_a_00907)
189. Gonzales MM, Tarumi T, Mumford JA, Ellis RC, Hungate JR, Pyron M, Tanaka H, Haley AP. 2014 Greater BOLD response to working memory in endurance-trained adults revealed by breath-hold calibration. *Hum. Brain Mapp.* **35**, 2898–2910. (doi:10.1002/hbm.22372)
190. Kannurpatti SS, Motes MA, Rypma B, Biswal BB. 2011 Increasing measurement accuracy of age-related BOLD signal change: minimizing vascular contributions by resting-state-fluctuation-of-amplitude scaling. *Hum. Brain Mapp.* **32**, 1125–1140. (doi:10.1002/hbm.21097)
191. Kannurpatti SS, Motes MA, Rypma B, Biswal BB. 2010 Neural and vascular variability and the fMRI-BOLD response in normal aging. *Magn. Reson. Imaging* **28**, 466–476. (doi:10.1016/j.mri.2009.12.007)
192. Mayhew SD, Li S, Storrar JK, Tsvetanov KA, Kourtzi Z. 2010 Learning shapes the representation of visual categories in the aging human brain. *J. Cogn. Neurosci.* **22**, 2899–2912. (doi:10.1162/jocn.2010.21415)
193. Mayhew SD, Kourtzi Z. 2013 Dissociable circuits for visual shape learning in the young and aging human brain. *Front. Hum. Neurosci.* **7**, 1–15. (doi:10.3389/fnhum.2013.00075)
194. Riecker A, Grodd W, Klose U, Schulz JB, Gröschel K, Erb M, Ackermann H, Kastrup A. 2003 Relation between regional functional MRI activation and vascular reactivity to carbon dioxide during normal aging. *J. Cereb. Blood Flow Metab.* **23**, 565–573. (doi:10.1097/01.WCB.0000056063.25434.04)
195. Mayhew SD, Macintosh BJ, Dirckx SG, Iannetti GD, Wise RG. 2010 Coupling of simultaneously acquired electrophysiological and haemodynamic responses during visual stimulation. *Magn. Reson. Imaging* **28**, 1066–1077. (doi:10.1016/j.mri.2010.03.027)
196. Raut RV, Nair VA, Sattin JA, Prabhakaran V. 2016 Hypercapnic evaluation of vascular reactivity in healthy aging and acute stroke via functional MRI. *NeuroImage Clin.* **12**, 173–179. (doi:10.1016/j.nicl.2016.06.016)
197. Jahanian H, Christen T, Moseley ME, Pajewski NM, Wright CB, Tamura MK, Zaharchuk G, for the SPRINT Study Research Group. 2017 Measuring vascular reactivity with resting-state blood oxygenation level-dependent (BOLD) signal fluctuations: a potential alternative to the breath-holding challenge? *J. Cereb. Blood Flow Metab.* **37**, 2526–2538. (doi:10.1177/0271678X16670921)
198. Golestani AM, Chang C, Kwinta JB, Khatamian YB, Jean Chen J. 2015 Mapping the end-tidal CO_2 response function in the resting-state BOLD fMRI signal: spatial specificity, test–retest reliability and effect of fMRI sampling rate. *NeuroImage* **104**, 266–277. (doi:10.1016/j.neuroimage.2014.10.031)
199. Wise RG, Ide K, Poulin MJ, Tracey I. 2004 Resting fluctuations in arterial carbon dioxide induce significant low frequency variations in BOLD signal. *NeuroImage* **21**, 1652–1664. (doi:10.1016/j.neuroimage.2003.11.025)
200. Kannurpatti SS, Biswal BB. 2008 Detection and scaling of task-induced fMRI-BOLD response using resting state fluctuations. *NeuroImage* **40**, 1567–1574. (doi:10.1016/j.neuroimage.2007.09.040)
201. Garrett DD, Lindenberger U, Hoge RD, Gauthier CJ. 2017 Age differences in brain signal variability are robust to multiple vascular controls. *Sci. Rep.* **7**, 10149. (doi:10.1038/s41598-017-09752-7)
202. Liu P, Hebrank AC, Rodrigue KM, Kennedy KM, Park DC, Lu H. 2013 A comparison of physiologic modulators of fMRI signals. *Hum. Brain Mapp.* **35**, 2078–2088. (doi:10.1002/hbm.22053)
203. De Vis JB, Bhogal AA, Hendrikse J, Petersen ET, Siero JCW. 2018 Effect sizes of BOLD CVR, resting-state signal fluctuations and time delay measures for the assessment of hemodynamic impairment in carotid occlusion patients. *NeuroImage* **179**, 530–539. (doi:10.1016/j.neuroimage.2018.06.017)
204. Jahanian H, Ni WW, Christen T, Moseley ME, Kurella Tamura M, Zaharchuk G. 2014 Spontaneous BOLD signal fluctuations in young healthy subjects and elderly patients with chronic kidney disease. *PLoS ONE* **9**, e92539. (doi:10.1371/journal.pone.0092539)
205. Kumral D, Şansal F, Cesnaite E, Mahjoory K, Al E, Gaebler M, Nikulin VV, Villringer A. 2019 BOLD and EEG signal variability at rest differently relate to aging in the human brain. *bioRxiv* 646273. (doi:10.1101/646273)
206. Chang C, Metzger CD, Glover GH, Duyn JH, Heinze H-J, Walter M. 2013 Association between heart rate variability and fluctuations in resting-state functional connectivity. *NeuroImage* **68**, 93–104. (doi:10.1016/j.neuroimage.2012.11.038)
207. Chang C, Cunningham JP, Glover GH. 2009 Influence of heart rate on the BOLD signal: the cardiac response function. *NeuroImage* **44**, 857–869. (doi:10.1016/j.neuroimage.2008.09.029)
208. Nair VA, Raut RV, Prabhakaran V. 2017 Investigating the blood oxygenation level-dependent functional MRI response to a verbal fluency task in early stroke before and after hemodynamic scaling. *Front. Neurol.* **8**, 283. (doi:10.3389/fneur.2017.00283)
209. Mill RD, Gordon BA, Balota DA, Cole MW. 2020 Predicting dysfunctional age-related task activations from resting-state network alterations. *NeuroImage* **221**, 117167. (doi:10.1016/j.neuroimage.2020.117167)
210. Mayhew SD, Mullinger KJ, Ostwald D, Porcaro C, Bowtell R, Bagshaw AP, Francis ST. 2016 Global signal modulation of single-trial fMRI response variability: effect on positive vs negative BOLD response relationship. *NeuroImage* **133**, 62–74. (doi:10.1016/j.neuroimage.2016.02.077)
211. Kannurpatti SS, Motes MA, Biswal BB, Rypma B. 2014 Assessment of unconstrained cerebrovascular reactivity marker for large age-range fMRI studies. *PLoS ONE* **9**, e88751. (doi:10.1371/journal.pone.0088751)
212. Boyke J, Driemeyer J, Gaser C, Büchel C, May A. 2008 Training-induced brain structure changes in the elderly. *J. Neurosci.* **28**, 7031–7035. (doi:10.1523/JNEUROSCI.0742-08.2008)
213. Rowe JB, Siebner H, Filipovic SR, Cordivari C, Gerschlager W, Rothwell J, Frackowiak R. 2006 Aging is associated with contrasting changes in local and distant cortical connectivity in the human motor system. *NeuroImage* **32**, 747–760. (doi:10.1016/j.neuroimage.2006.03.061)
214. Scholz J, Klein MC, Behrens TEJ, Johansen-Berg H. 2009 Training induces changes in white-matter architecture. *Nat. Neurosci.* **12**, 1370–1371. (doi:10.1038/nn.2412)
215. Tigges J, Herndon JG, Peters A. 1990 Neuronal population of area 4 during the life span of the

rhesus monkey. *Neurobiol. Aging* **11**, 201–208. (doi:10.1016/0197-4580(90)90546-C)

216. Liu P, Li Y, Pinho M, Park DC, Welch BG, Lu H. 2017 Cerebrovascular reactivity mapping without gas challenges. *NeuroImage* **146**, 320–326. (doi:10.1016/j.neuroimage.2016.11.054)
217. Kazan SM, Mohammadi S, Callaghan MF, Flandin G, Huber L, Leech R, Kennerley A, Windischberger C, Weiskopf N. 2016 Vascular autorescaling of fMRI (VasA fMRI) improves sensitivity of population studies: a pilot study. *NeuroImage* **124**, 794–805. (doi:10.1016/j.neuroimage.2015.09.033)
218. Sami S, Robertson EM, Miall RC. 2014 The time course of task-specific memory consolidation effects in resting state networks. *J. Neurosci.* **34**, 3982–3992. (doi:10.1523/JNEUROSCI.4341-13.2014)
219. Sami S, Miall RC. 2013 Graph network analysis of immediate motor-learning induced changes in resting state BOLD. *Front. Hum. Neurosci.* **7**, 166. (doi:10.3389/fnhum.2013.00166)
220. Lu H, Yezhuvath US, Xiao G. 2010 Improving fMRI sensitivity by normalization of basal physiologic state. *Hum. Brain Mapp.* **31**, 80–87. (doi:10.1002/hbm.20846)
221. Bright MG, Croal PL, Blockley NP, Bulte DP. 2019 Multiparametric measurement of cerebral physiology using calibrated fMRI. *NeuroImage* **187**, 128–144. (doi:10.1016/j.neuroimage.2017.12.049)
222. Blockley NP, Griffeth VEM, Simon AB, Dubowitz DJ, Buxton RB. 2015 Calibrating the BOLD response without administering gases: comparison of hypercapnia calibration with calibration using an asymmetric spin echo. *NeuroImage* **104**, 423–429. (doi:10.1016/j.neuroimage.2014.09.061)
223. Pike GB. 2012 Quantitative functional MRI: concepts, issues and future challenges. *NeuroImage* **62**, 1234–1240. (doi:10.1016/j.neuroimage.2011.10.046)
224. Gauthier CJ, Fan AP. 2019 BOLD signal physiology: models and applications. *NeuroImage* **187**, 116–127. (doi:10.1016/j.neuroimage.2018.03.018)
225. Gauthier CJ, Hoge RD. 2012 Magnetic resonance imaging of resting OEF and $CMRO_2$ using a generalized calibration model for hypercapnia and hyperoxia. *NeuroImage* **60**, 1212–1225. (doi:10.1016/j.neuroimage.2011.12.056)
226. Ances BM, Liang CL, Leontiev O, Perthen JE, Fleisher AS, Lansing AE, Buxton RB. 2009 Effects of aging on cerebral blood flow, oxygen metabolism, and blood oxygenation level dependent responses to visual stimulation. *Hum. Brain Mapp.* **30**, 1120–1132. (doi:10.1002/hbm.20574)
227. Hutchison JL, Shokri-Kojori E, Lu H, Rypma B. 2013 A BOLD perspective on age-related neurometabolic-flow coupling and neural efficiency changes in human visual cortex. *Front. Psychol.* **4**, 244. (doi:10.3389/fpsyg.2013.00244)
228. Mohtasib RS, Lumley G, Goodwin JA, Emsley HCA, Sluming V, Parkes LM. 2012 Calibrated fMRI during a cognitive Stroop task reveals reduced metabolic response with increasing age. *NeuroImage* **59**, 1143–1151. (doi:10.1016/j.neuroimage.2011.07.092)
229. Neubauer AC, Fink A. 2009 Intelligence and neural efficiency. *Neurosci. Biobehav. Rev.* **33**, 1004–1023. (doi:10.1016/j.neubiorev.2009.04.001)
230. Rypma B, Eldreth DA, Rebbechi D. 2007 Age-related differences in activation–performance relations in delayed-response tasks: a multiple component analysis. *Cortex* **43**, 65–76. (doi:10.1016/s0010-9452(08)70446-5)
231. Rypma B, Berger JS, Genova HM, Rebbechi D, D'Esposito M. 2005 Dissociating age-related changes in cognitive strategy and neural efficiency using event-related fMRI. *Cortex* **41**, 582–594. (doi:10.1016/S0010-9452(08)70198-9)
232. He B, Sohrabpour A, Brown E, Liu Z. 2018 Electrophysiological source imaging: a noninvasive window to brain dynamics. *Annu. Rev. Biomed. Eng.* **20**, 171–196. (doi:10.1146/annurev-bioeng-062117-120853)
233. Sotero RC, Trujillo-Barreto NJ. 2008 Biophysical model for integrating neuronal activity, EEG, fMRI and metabolism. *NeuroImage* **39**, 290–309. (doi:10.1016/j.neuroimage.2007.08.001)
234. Laufs H. 2008 Endogenous brain oscillations and related networks detected by surface EEG-combined fMRI. *Hum. Brain Mapp.* **29**, 762–769. (doi:10.1002/hbm.20600)
235. Ritter P, Villringer A. 2006 Simultaneous EEG–fMRI. *Neurosci. Biobehav. Rev.* **30**, 823–838. (doi:10.1016/j.neubiorev.2006.06.008)
236. He B, Liu Z. 2008 Multimodal functional neuroimaging: integrating functional MRI and EEG/MEG. *IEEE Rev. Biomed. Eng.* **1**, 23–40. (doi:10.1109/RBME.2008.2008233)
237. Henson RN, Wakeman DG, Litvak V, Friston KJ. 2011 A parametric empirical Bayesian framework for the EEG/MEG inverse problem: generative models for multi-subject and multi-modal integration. *Front. Hum. Neurosci.* **5**, 76. (doi:10.3389/fnhum.2011.00076) https://doi.org/10.3389/fnhum.2011.00076.
238. Lauritzen M, Gold L. 2003 Brain function and neurophysiological correlates of signals used in functional neuroimaging. *J. Neurosci.* **23**, 3972–3980. (doi:10.1523/jneurosci.23-10-03972.2003)
239. Logothetis NK, Pauls J, Augath M, Trinath T, Oeltermann A. 2001 Neurophysiological investigation of the basis of the fMRI signal. *Nature* **412**, 150–157. (doi:10.1038/news010712-13)
240. Viswanathan A, Freeman RD. 2007 Neurometabolic coupling in cerebral cortex reflects synaptic more than spiking activity. *Nat. Neurosci.* **10**, 1308–1312. (doi:10.1038/nn1977)
241. Brookes MJ, Woolrich M, Luckhoo H, Price D, Hale JR, Stephenson MC, Barnes GR, Smith SM, Morris PG. 2011 Investigating the electrophysiological basis of resting state networks using magnetoencephalography. *Proc. Natl Acad. Sci. USA* **108**, 16783–16788. (doi:10.1073/pnas.1112685108)
242. Hipp JF, Siegel M. 2015 BOLD fMRI correlation reflects frequency-specific neuronal correlation. *Curr. Biol.* **25**, 1368–1374. (doi:10.1016/j.cub.2015.03.049)
243. Scheeringa R, Fries P, Petersson K-M, Oostenveld R, Grothe I, Norris DG, Hagoort P, Bastiaansen MCM. 2011 Neuronal dynamics underlying high- and low-frequency EEG oscillations contribute independently to the human BOLD signal. *Neuron* **69**, 572–583. (doi:10.1016/j.neuron.2010.11.044)
244. Wen H, Liu Z. 2016 Broadband electrophysiological dynamics contribute to global resting-state fMRI signal. *J. Neurosci.* **36**, 6030–6040. (doi:10.1523/JNEUROSCI.0187-16.2016)
245. Bruffaerts R, Tyler LK, Shafto M, Tsvetanov KA, Clarke A. 2019 Perceptual and conceptual processing of visual objects across the adult lifespan. *Sci. Rep.* **9**, 13771. (doi:10.1038/s41598-019-50254-5)
246. Lin M-Y, Tseng Y-J, Cheng C-H. 2018 Age effects on spatiotemporal dynamics of response inhibition: an MEG study. *Front. Aging Neurosci.* **10**, 1–9. (doi:10.3389/fnagi.2018.00386)
247. Moran RJ, Symmonds M, Dolan RJ, Friston KJ. 2014 The brain ages optimally to model its environment: evidence from sensory learning over the adult lifespan. *PLoS Comput. Biol.* **10**, e1003422. (doi:10.1371/journal.pcbi.1003422)
248. Price D *et al.* 2017 Age-related delay in visual and auditory evoked responses is mediated by white- and grey-matter differences. *Nat. Commun.* **8**, 15671. (doi:10.1038/ncomms15671)
249. Susi G *et al.* 2019 Healthy and pathological neurocognitive aging: spectral and functional connectivity analyses using magnetoencephalography. In *Oxford Research Encyclopedia of Psychology*. New York, NY: Oxford University Press. https://doi.org/10.1093/acrefore/9780190236557.013.387.
250. Stickland R, Allen M, Magazzini L, Singh KD, Wise RG, Tomassini V. 2019 Neurovascular coupling during visual stimulation in multiple sclerosis: a MEG-fMRI study. *Neuroscience* **403**, 54–69. (doi:10.1016/j.neuroscience.2018.03.018)
251. Mullinger KJ, Mayhew SD, Bagshaw AP, Bowtell R, Francis ST. 2013 Poststimulus undershoots in cerebral blood flow and BOLD fMRI responses are modulated by poststimulus neuronal activity. *Proc. Natl Acad. Sci. USA* **110**, 13 636–13 641. (doi:10.1073/pnas.1221287110)
252. Allen PJ, Josephs O, Turner R. 2000 A method for removing imaging artifact from continuous EEG recorded during functional MRI. *NeuroImage* **12**, 230–239. (doi:10.1006/nimg.2000.0599)
253. Balsters JH *et al.* 2013 Changes in resting connectivity with age: a simultaneous electroencephalogram and functional magnetic resonance imaging investigation. *Neurobiol. Aging* **34**, 2194–2207. (doi:10.1016/j.neurobiolaging.2013.03.004)
254. Ahlfors SP, Han J, Belliveau JW, Hämäläinen MS. 2010 Sensitivity of MEG and EEG to source orientation. *Brain Topogr.* **23**, 227–232. (doi:10.1007/s10548-010-0154-x)
255. Krishnaswamy P, Obregon-Henao G, Ahveninen J, Khan S, Babadi B, Iglesias JE, Hämäläinen MS, Purdon PL. 2017 Sparsity enables estimation of

both subcortical and cortical activity from MEG and EEG. *Proc. Natl Acad. Sci. USA* **114**, E10465–E10474. (doi:10.1073/pnas.1705414114)

256. Muthuraman M, Moliadze V, Mideksa KG, Anwar AR, Stephani U, Deuschl G, Freitag CM, Siniatchkin M. 2015 EEG-MEG integration enhances the characterization of functional and effective connectivity in the resting state network. *PLoS ONE* **10**, e0140832. (doi:10.1371/journal.pone.0140832)
257. Thompson GJ, Riedl V, Grimmer T, Drzezga A, Herman P, Hyder F. 2016 The whole-brain 'global' signal from resting state fMRI as a potential biomarker of quantitative state changes in glucose metabolism. *Brain Connect.* **6**, 435–447. (doi:10.1089/brain.2015.0394)
258. Devous M, Kennedy K, Rodrigue K, Hebrank A, Park D. 2012 Beta-amyloid burden alters default mode and salience network connectivity associated with impaired cognition in healthy aging. *Alzheimers Dement.* **8**, P67. (doi:10.1016/j.jalz.2012.05.159)
259. Chen MK *et al.* 2018 Assessing synaptic density in Alzheimer disease with synaptic vesicle glycoprotein 2A positron emission tomographic imaging. *JAMA Neurol.* **75**, 1215–1224. (doi:10.1001/jamaneurol.2018.1836)
260. Fabiani M *et al.* 2014 Neurovascular coupling in normal aging: a combined optical, ERP and fMRI study. *NeuroImage* **85**(Pt 1), 592–607. (doi:10.1016/j.neuroimage.2013.04.113)
261. Malpetti M *et al.* 2019 Microglial activation and tau burden predict cognitive decline in Alzheimer's disease. *medRxiv* 19011189. (doi:10.1101/19011189)
262. Passamonti L *et al.* 2019 Neuroinflammation and functional connectivity in Alzheimer's disease: interactive influences on cognitive performance. *J. Neurosci.* **39**, 2574–2518. (doi:10.1523/JNEUROSCI.2574-18.2019)
263. Kantarci K *et al.* 2010 MRS in presymptomatic MAPT mutation carriers: a potential biomarker for tau-mediated pathology. *Neurology* **75**, 771–778. (doi:10.1212/WNL.0b013e3181f073c7)
264. Murley AG, Rowe JB. 2018 Neurotransmitter deficits from frontotemporal lobar degeneration. *Brain* **141**, 1263–1285. (doi:10.1093/brain/awx327)
265. Davis SW, Luber B, Murphy DLK, Lisanby SH, Cabeza R. 2017 Frequency-specific neuromodulation of local and distant connectivity in aging and episodic memory function. *Hum. Brain Mapp.* **38**, 5987–6004. (doi:10.1002/hbm.23803)
266. Tan J, Iyer KK, Tang AD, Jamil A, Martins RN, Sohrabi HR, Nitsche MA, Hinder MR, Fujiyama H. 2019 Modulating functional connectivity with non-invasive brain stimulation for the investigation and alleviation of age-associated declines in response inhibition: a narrative review. *NeuroImage* **185**, 490–512. (doi:10.1016/j.neuroimage.2018.10.044)
267. Buxton RB, Wong EC, Frank LR. 1998 Dynamics of blood flow and oxygenation changes during brain activation: the balloon model. *Magn. Reson. Med.* **39**, 855–864. (doi:10.1002/mrm.1910390602)
268. Friston KJ, Mechelli A, Turner R, Price CJ. 2000 Nonlinear responses in fMRI: the balloon model, Volterra kernels, and other hemodynamics. *NeuroImage* **12**, 466–477. (doi:10.1006/nimg.2000.0630)
269. Menon RS. 2012 The great brain versus vein debate. *NeuroImage* **62**, 970–974. (doi:10.1016/j.neuroimage.2011.09.005)
270. Elbau IG *et al.* 2018 The brain's hemodynamic response function rapidly changes under acute psychosocial stress in association with genetic and endocrine stress response markers. *Proc. Natl Acad. Sci. USA* **115**, E10206–E10215. (doi:10.1073/pnas.1804340115)
271. Shan ZY *et al.* 2016 Genes influence the amplitude and timing of brain hemodynamic responses. *NeuroImage* **124**, 663–671. (doi:10.1016/j.neuroimage.2015.09.016)
272. Tong Y, Yao J(F), Chen JJ, Frederick BdB. 2019 The resting-state fMRI arterial signal predicts differential blood transit time through the brain. *J. Cereb. Blood Flow Metab.* **39**, 1148–1160. (doi:10.1177/0271678X17753329)
273. Handwerker DA, Ollinger JM, D'Esposito M. 2004 Variation of BOLD hemodynamic responses across subjects and brain regions and their effects on statistical analyses. *NeuroImage* **21**, 1639–1651. (doi:10.1016/j.neuroimage.2003.11.029)
274. Havlicek M, Uludağ K. 2020 A dynamical model of the laminar BOLD response. *NeuroImage* **204**, 116209. (doi:10.1016/j.neuroimage.2019.116209)
275. Taylor AJ, Kim JH, Ress D. 2018 Characterization of the hemodynamic response function across the majority of human cerebral cortex. *NeuroImage* **173**, 322–331. (doi:10.1016/j.neuroimage.2018.02.061)
276. Friston KJ, Josephs O, Rees G, Turner R. 1998 Nonlinear event-related responses in fMRI. *Magn. Reson. Med.* **39**, 41–52. (doi:10.1002/mrm.1910390109)
277. D'Esposito M, Zarahn E, Aguirre G, Rypma B. 1999 The effect of normal aging on the coupling of neural activity to the bold hemodynamic response. *NeuroImage* **10**, 6–14. (doi:10.1006/nimg.1999.0444)
278. Degras D, Lindquist MA. 2014 A hierarchical model for simultaneous detection and estimation in multi-subject fMRI studies. *NeuroImage* **98**, 61–72. (doi:10.1016/j.neuroimage.2014.04.052)
279. Pedregosa F, Eickenberg M, Ciuciu P, Thirion B, Gramfort A. 2015 Data-driven HRF estimation for encoding and decoding models. *NeuroImage* **104**, 209–220. (doi:10.1016/j.neuroimage.2014.09.060)
280. West KL, Zuppichini MD, Turner MP, Sivakolundu DK, Zhao Y, Abdelkarim D, Spence JS, Rypma B. 2019 BOLD hemodynamic response function changes significantly with healthy aging. *NeuroImage* **188**, 198–207. (doi:10.1016/j.neuroimage.2018.12.012)
281. Shafto *et al.* 2014 The Cambridge Centre for Ageing and Neuroscience (Cam-CAN) study protocol: a cross-sectional, lifespan, multidisciplinary examination of healthy cognitive ageing. *BMC Neurology* **14**, 204. (doi:10.1186/s12883-014-0204-1)
282. Friston KJ, Harrison L, Penny W. 2003 Dynamic causal modelling. *NeuroImage* **19**, 1273–1302. (doi:10.1016/S1053-8119(03)00202-7)
283. Razi A, Kahan J, Rees G, Friston KJ. 2015 Construct validation of a DCM for resting state fMRI. *NeuroImage* **106**, 1–14. (doi:10.1016/j.neuroimage.2014.11.027)
284. Daunizeau J, David O, Stephan KE. 2011 Dynamic causal modelling: a critical review of the biophysical and statistical foundations. *NeuroImage* **58**, 312–322. (doi:10.1016/j.neuroimage.2009.11.062)
285. McKeown MJ, Makeig S, Brown GG, Jung TP, Kindermann SS, Bell AJ, Sejnowski TJ. 1998 Analysis of fMRI data by blind separation into independent spatial components. *Hum. Brain Mapp.* **6**, 160–188. (doi:10.1002/(SICI)1097-0193(1998)6:3<160::AID-HBM5>3.0.CO;2-1)
286. Tong Y, Frederick BdB. 2014 Studying the spatial distribution of physiological effects on BOLD signals using ultrafast fMRI. *Front. Hum. Neurosci.* **8**, 1–8. (doi:10.3389/fnhum.2014.00196)
287. Kundu P, Voon V, Balchandani P, Lombardo MV, Poser BA, Bandettini PA. 2017 Multi-echo fMRI: a review of applications in fMRI denoising and analysis of BOLD signals. *NeuroImage* **154**, 59–80. (doi:10.1016/j.neuroimage.2017.03.033)
288. Campbell KL *et al.* 2015 Idiosyncratic responding during movie-watching predicted by age differences in attentional control. *Neurobiol. Aging* **36**, 3045–3055. (doi:10.1016/j.neurobiolaging.2015.07.028)
289. Tsvetanov KA, Ye Z, Hughes L, Samu D, Treder MS, Wolpe N, Tyler LK, Rowe JB, for Cambridge Centre for Ageing and Neuroscience. 2018 Activity and connectivity differences underlying inhibitory control across the adult lifespan. *J. Neurosci.* **38**, 7887–7900. (doi:10.1523/JNEUROSCI.2919-17.2018)
290. Xu J, Potenza MN, Calhoun VD. 2013 Spatial ICA reveals functional activity hidden from traditional fMRI GLM-based analyses. *Front. Neurosci.* **7**, 1–4. (doi:10.3389/fnins.2013.00154)
291. Aron AR, Poldrack Ra. 2006 Cortical and subcortical contributions to Stop signal response inhibition: role of the subthalamic nucleus. *J. Neurosci.* **26**, 2424–2433. (doi:10.1523/JNEUROSCI.4682-05.2006)
292. LeVan P, Gotman J. 2009 Independent component analysis as a model-free approach for the detection of BOLD changes related to epileptic spikes: a simulation study. *Hum. Brain Mapp.* **30**, 2021–2031. (doi:10.1002/hbm.20647)
293. Schöpf V *et al.* 2011 Model-free fMRI group analysis using FENICA. *NeuroImage* **55**, 185–193. (doi:10.1016/j.neuroimage.2010.11.010)
294. Samu D *et al.* 2017 Preserved cognitive functions with age are determined by domain-dependent shifts in network responsivity. *Nat. Commun.* **8**, 14743. (doi:10.1038/ncomms14743)
295. Bethlehem RAI, Paquola C, Seidlitz J, Ronan L, Bernhardt B, Cam-CAN Consortium, Tsvetanov KA. 2020 Dispersion of functional gradients across the adult lifespan. *NeuroImage*. **222**, 117299. (doi:10.1016/j.neuroimage.2020.117299)
296. Wardlaw JM *et al.* 2013 Neuroimaging standards for research into small vessel disease and its contribution to ageing and neurodegeneration.

Lancet Neurol. **12**, 822–838. (doi:10.1016/S1474-4422(13)70124-8)

297. Baumgart M, Snyder HM, Carrillo MC, Fazio S, Kim H, Johns H. 2015 Summary of the evidence on modifiable risk factors for cognitive decline and dementia: a population-based perspective. *Alzheimers Dement.* **11**, 718–726. (doi:10.1016/j.jalz.2015.05.016)
298. Puzo C *et al.* 2019 Independent effects of white matter hyperintensities on cognitive, neuropsychiatric, and functional decline: a longitudinal investigation using the National Alzheimer's Coordinating Center Uniform Data Set. *Alzheimers Res. Ther.* **11**, 64. (doi:10.1186/s13195-019-0521-0)
299. Stefanidis KB, Askew CD, Klein T, Lagopoulos J, Summers MJ. 2019 Healthy aging affects cerebrovascular reactivity and pressure-flow responses, but not neurovascular coupling: a cross-sectional study. *PLoS ONE* **14**, e0217082. (doi:10.1371/journal.pone.0217082)
300. Barnes JN. 2015 Exercise, cognitive function, and aging. *Adv. Physiol. Educ.* **39**, 55–62. (doi:10.1152/advan.00101.2014)
301. Kisler K, Nelson AR, Montagne A, Zlokovic BV. 2017 Cerebral blood flow regulation and neurovascular dysfunction in Alzheimer disease. *Nat. Rev. Neurosci.* **18**, 419–434. (doi:10.1038/nrn.2017.48)
302. Tsvetanov KA *et al.* 2020 Brain functional network integrity sustains cognitive function despite atrophy in presymptomatic genetic frontotemporal dementia. *Alzheimer's Dement.* 1–15. (doi:10.1002/alz.12209)
303. Boekel W, Wagenmakers E-J, Belay L, Verhagen J, Brown S, Forstmann BU. 2015 A purely confirmatory replication study of structural brain–behavior correlations. *Cortex* **66**, 115–133. (doi:10.1016/j.cortex.2014.11.019)
304. Shafto MA *et al.* 2019 Cognitive diversity in a healthy aging cohort: cross-domain cognition in the Cam-CAN Project. *J. Aging Health* **66**, 115–133. (doi:10.1177/0898264319878095)
305. Small BJ, Dixon RA, McArdle JJ. 2011 Tracking cognition–health changes from 55 to 95 years of age. *J. Gerontol. B Psychol. Sci. Soc. Sci.* **66**(Suppl. 1), i153–i161. (doi:10.1093/geronb/gbq093)
306. Grady C. 2012 The cognitive neuroscience of ageing. *Nat. Rev. Neurosci.* **13**, 491–505. (doi:10.1038/nrn3256)
307. Park DC, Polk TA, Park R, Minear M, Savage A, Smith MR. 2004 Aging reduces neural specialization in ventral visual cortex. *Proc. Natl. Acad. Sci. USA* **101**, 13 091–13 095. (doi:10.1073/pnas.0405148101)
308. Cabeza R *et al.* 2018 Maintenance, reserve and compensation: the cognitive neuroscience of healthy ageing. *Nat. Rev. Neurosci.* **19**, 701–710. (doi:10.1038/s41583-018-0068-2)
309. Morcom AM, Johnson W. 2015 Neural reorganization and compensation in aging. *J. Cogn. Neurosci.* **27**, 1275–1285. (doi:10.1162/jocn_a_00783)
310. Lederer DJ *et al.* 2019 Control of confounding and reporting of results in causal inference studies. *Ann. Am. Thorac. Soc.* **16**, 22–28. (doi:10.1513/AnnalsATS.201808-564PS)
311. Lindquist MA, Geuter S, Wager TD, Caffo BS. 2019 Modular preprocessing pipelines can reintroduce artifacts into fMRI data. *Hum. Brain Mapp.* **40**, 2358–2376. (doi:10.1002/hbm.24528)